

MARTIN MARIETTA ENERGY SYSTEMS LIBRARIES



3 4456 0286161 4

CENTRAL RESEARCH LIBRARY  
DOCUMENT COLLECTION

ORNL-3152  
UC-4 - Chemistry

RADIOACTIVITY OF NUCLEAR REACTOR  
COOLING FLUIDS

J. C. Ward

CENTRAL RESEARCH LIBRARY  
DOCUMENT COLLECTION

**LIBRARY LOAN COPY**

**DO NOT TRANSFER TO ANOTHER PERSON**

If you wish someone else to see this  
document, send in name with document  
and the library will arrange a loan.



**OAK RIDGE NATIONAL LABORATORY**

operated by

**UNION CARBIDE CORPORATION**

for the

**U.S. ATOMIC ENERGY COMMISSION**

Printed in USA. Price \$2.50. Available from the  
Office of Technical Services  
Department of Commerce  
Washington 25, D. C.

LEGAL NOTICE

This report was prepared as an account of Government sponsored work. Neither the United States, nor the Commission, nor any person acting on behalf of the Commission:

- A. Makes any warranty or representation, expressed or implied, with respect to the accuracy, completeness, or usefulness of the information contained in this report, or that the use of any information, apparatus, method, or process disclosed in this report may not infringe privately owned rights; or
  - B. Assumes any liabilities with respect to the use of, or for damages resulting from the use of any information, apparatus, method, or process disclosed in this report.
- As used in the above, "person acting on behalf of the Commission" includes any employee or contractor of the Commission, or employee of such contractor, to the extent that such employee or contractor of the Commission, or employee of such contractor prepares, disseminates, or provides access to, any information pursuant to his employment or contract with the Commission, or his employment with such contractor.

Contract No. W-7405-eng-26

ANALYTICAL CHEMISTRY DIVISION

RADIOACTIVITY OF NUCLEAR REACTOR COOLING FLUIDS

J. C. Ward

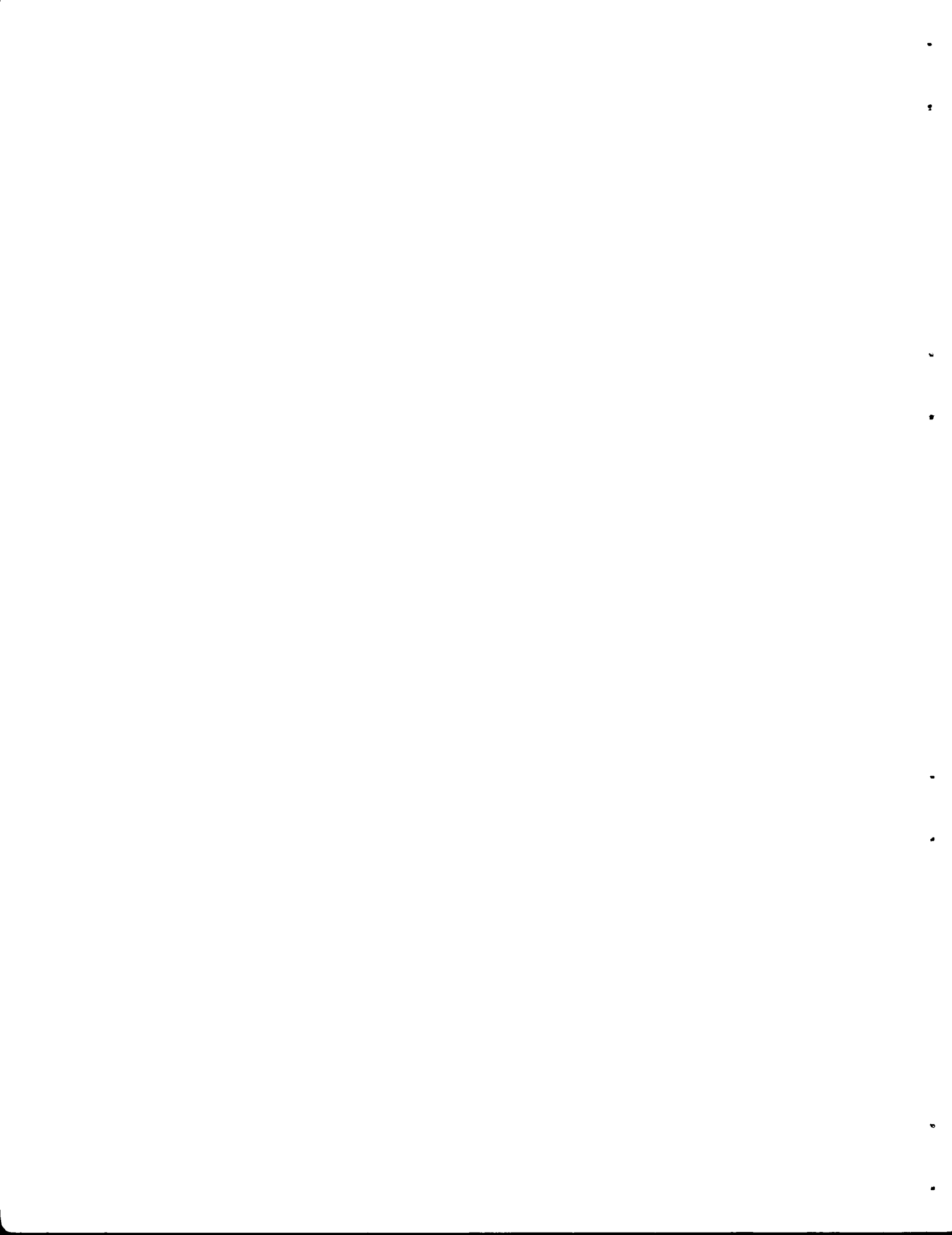
DATE ISSUED

SEP 20 1961

Submitted as a thesis to the Graduate Council of the University of Oklahoma in partial fulfillment of the requirements for the degree of Doctor of Philosophy

OAK RIDGE NATIONAL LABORATORY  
Oak Ridge, Tennessee  
operated by  
UNION CARBIDE CORPORATION  
for the  
U. S. ATOMIC ENERGY COMMISSION





## ACKNOWLEDGMENTS

This report is based upon a thesis submitted to the University of Oklahoma in partial fulfillment of the requirements for the doctoral degree. The report describes research carried out in the Analytical Chemistry Division at the Oak Ridge National Laboratory.

The research was supported by the Oak Ridge Graduate Fellowship Program of the Oak Ridge Institute of Nuclear Studies and was directed by a committee appointed by Dean Lloyd E. Swearingen of the University of Oklahoma Graduate School which was composed of Dr. G. W. Reid and Dr. R. A. Howard of the Department of Civil Engineering at the University of Oklahoma and Dr. M. T. Kelley and Mr. G. W. Leddicotte of the Analytical Chemistry Division of the Oak Ridge National Laboratory.

TABLE OF CONTENTS

	Page
LIST OF TABLES . . . . .	vi
LIST OF ILLUSTRATIONS . . . . .	viii
LIST OF GRAPHS . . . . .	ix
Chapter	
I. INTRODUCTION . . . . .	1
Neutron Induced Activities in Cooling Fluids Containing Oxygen . . . . .	2
The Importance of Water Cooled Nuclear Reactors . . . . .	4
II. DESCRIPTION OF EXPERIMENTAL FACILITIES . . . . .	6
General Description of the Oak Ridge National Laboratory Research Reactor . . . . .	6
Ion Exchange System of the ORR . . . . .	8
III. EXPERIMENTAL RESULTS . . . . .	13
A Method for the Analysis of Dissolved Gases in Water . . . . .	13
Analysis of the Demineralized Make-Up Water . . . . .	16
Concentration of Stable Elements in the Cooling Water . . . . .	17
Method of Analysis of Cooling Water for Radioactive Isotopes . . . . .	17
Measured Concentrations of Radioactive Isotopes in the Cooling Water . . . . .	21
Measurement of $N^{17}$ in the Cooling Water . . . . .	33
Argon . . . . .	35
Removal of Active Nuclides by Ion Exchange . . . . .	38
Recoil Mechanism Study . . . . .	43
IV. THEORY . . . . .	47
Derivation of the Equilibrium Equations for Nuclear Reactor Cooling Fluids . . . . .	47
The Non-Equilibrium Equation . . . . .	51
Activity Attributable to Recoil Mechanism . . . . .	53

TABLE OF CONTENTS (Continued)

	Page
Integration of the Fission Neutron	
Spectrum Integral . . . . .	63
Effective Retention Time . . . . .	70
Burnup Effects . . . . .	71
V. CONCLUSIONS . . . . .	72
Non-Equilibrium Equation Verification . . . . .	72
Origin of the Na <sup>24</sup> Activity . . . . .	75
Origin of the Cadmium Activity . . . . .	76
Origin of Fission Products . . . . .	77
Possibility of Detecting Fuel Element	
Rupture by Measurement of Delayed	
Neutrons . . . . .	81
Recoil Mechanism . . . . .	86
Compensation of Burnup of U <sup>235</sup> Contamina-	
tion by Shim Rod Movement . . . . .	93
Effective Fission Flux Retention Time . . . . .	97
Effective Thermal Flux Retention Time . . . . .	97
Summary . . . . .	100
BIBLIOGRAPHY . . . . .	102
APPENDIX . . . . .	106

LIST OF TABLES

Table	Page
I. NUCLEAR REACTOR COOLANTS . . . . .	5
II. CHARACTERISTICS OF THE OAK RIDGE NATIONAL LABORATORY RESEARCH REACTOR . . . . .	7
III. CHEMICAL COMPOSITION OF THE ORR COOLING WATER . . . . .	18
IV. VALUES FOR THE DETERMINATION OF ABSORBER THICKNESS WITH $\text{Na}^{24}$ . . . . .	26
V. FUNDAMENTAL DATA USED . . . . .	28
VI. CONCENTRATION OF RADIOACTIVE ISOTOPES IN THE COOLING WATER . . . . .	30
VII. RATE OF PRODUCTION OF RADIOACTIVE ISOTOPES IN THE COOLING WATER . . . . .	32
VIII. DECREASE OF THE ACTIVITY OF $\text{A}^{41}$ WITH TIME . . . . .	36
IX. RESULTS OF THE ION EXCHANGE EXPERIMENTATION . . . . .	40
X. EFFICIENCY OF ION EXCHANGE . . . . .	44
XI. COEFFICIENTS FOR THE DETERMINATION OF $E_e - E_T$ . . . . .	62
XII. VALUES OF THE ERROR FUNCTION . . . . .	69
XIII. BUILDUP OF $\text{Na}^{24}$ IN THE REACTOR COOLING WATER . . . . .	73
XIV. PROPERTIES OF DELAYED NEUTRONS IN SLOW- NEUTRON FISSION OF URANIUM-235 . . . . .	83
XV. THERMAL AND FISSION NEUTRON CROSS SECTIONS FOR SEVERAL IMPORTANT REACTIONS . . . . .	87
XVI. PERCENT ABUNDANCE AND ATOMIC WEIGHT OF SEVERAL ISOTOPES . . . . .	89
XVII. VALUES OF $Q$ , $E_T$ , AND $E_e$ FOR SEVERAL FISSION NEUTRON REACTIONS . . . . .	90
XVIII. RECOIL RANGES . . . . .	92

LIST OF TABLES (Continued)

Tables	Page
XIX. OBSERVED AND CALCULATED RATES OF PRODUCTION OF Na <sup>24</sup> AND Mg <sup>27</sup> IN THE COOLING WATER . . . . .	94
XX. BUILDUP OF La <sup>140</sup> IN THE REACTOR COOLING WATER . . . . .	96
XXI. REQUIRED EFFECTIVE THERMAL NEUTRON FLUX RETENTION TIMES FOR SEVERAL RADIOACTIVE ISOTOPES . . . . .	99

LIST OF ILLUSTRATIONS

Illustration	Page
1. Reactor Cooling System . . . . .	9
2. ORNL Research Reactor Vertical Section . . . . .	10
3. Oak Ridge Research Reactor . . . . .	11

LIST OF GRAPHS

Graph	Page
1. Buildup of $\text{Na}^{24}$ in the Reactor Cooling Water . . . . .	74

# RADIOACTIVITY OF NUCLEAR REACTOR COOLING FLUIDS

## CHAPTER I

### INTRODUCTION

Most of the work that has been done with regard to nuclear reactor cooling fluids has been mainly of a qualitative nature. However, the most meaningful results from the standpoint of gamma-ray shielding are quantitative data. The main emphasis of the investigation described herein has been in the quantitative area.

In order to be meaningful, the results of a study on nuclear reactor cooling fluids should lead to analytical methods whereby the specific activities of the various radioactive isotopes in a nuclear reactor cooling system can be predicted. To accomplish this end on a sound basis, it is necessary to understand the method of formation of each radioactive isotope of interest. Equally important is the method or methods of removal of each radioactive isotope from the coolant.

Although this work is intended to be as complete in itself as possible, it will be readily apparent that more research in several areas is urgently needed. However, from the results of the work carried out, it should be possible to predict the specific activities of the more important radioactive isotopes in the cooling systems of nuclear reactors.

Radioactive isotopes are formed in reactor cooling systems by one or more of the following methods: (1) activation of the coolant itself, (2) activation of impurities in the coolant, (3) recoil of radioactive isotopes into the coolant from materials used in the reactor core,

(4) leakage of fission products from the reactor fuel elements, and (5) recoil of fission products into the coolant from surface contamination of the fuel element cladding.<sup>1</sup> All of these methods and the part they play in contributing to the specific activity of the coolant will be examined in some detail in the following discussion.

Although this entire investigation is concerned with closed cycle cooling systems, there should be no difficulty in applying the appropriate parts of the discussion to "once-through"<sup>2</sup> cooling systems. The reason for this emphasis on closed cycle systems is that some of the discussion will apply to once-through cooling systems, whereas the converse would not be true.

### Neutron Induced Activities in Cooling

#### Fluids Containing Oxygen

It is known that when oxygen or a compound containing oxygen is exposed to neutrons, reactions occur with all three oxygen isotopes

$O^{16}$  (99.76%),  $O^{17}$  (0.039%), and  $O^{18}$  (0.204%), as follows:<sup>3</sup>

(1)  $O^{16}(n,\alpha)C^{13}$  - 2.20 Mev:  $C^{13}$  is stable

(2)  $O^{16}(n,2n)O^{15}$  - 15.6 Mev:  $O^{15} \xrightarrow[118 \text{ s}]{\beta^+} N^{15}$

✓ (3)  $O^{16}(n,p)N^{16}$  - 9.5 Mev:  $N^{16} \xrightarrow[7.35 \text{ s}]{\beta^-} O^{16*} \xrightarrow[\text{inst.}]{\gamma} O^{16}$

<sup>1</sup>Some of the impurities in the coolant may well be corrosion products.

<sup>2</sup>"Once-through" cooling systems are cooling systems where the coolant is passed through the reactor core only one time.

<sup>3</sup>N. Faull, An Experimental Study of Neutron Induced Activities in Water, Atomic Energy Research Establishment Report Number 1919, (Harwell, Berks., England: 1957).

- (4)  $O^{17}(n,\alpha)C^{14} + 1.83 \text{ Mev: } C^{14} \xrightarrow[5600 \text{ y}]{\beta^-} N^{14}$
- (5)  $O^{17}(n,p)N^{17} - 8.0 \text{ Mev: } N^{17} \xrightarrow[4.14 \text{ s}]{\beta^-} O^{17} \xrightarrow[\text{inst.}]{n} O^{16}$
- (6)  $O^{18}(n,\gamma)O^{19} + 4.24 \text{ Mev: } O^{19} \xrightarrow[29.4 \text{ s}]{\beta^-} F^{19*} \xrightarrow[\text{inst.}]{\gamma} F^{19}$

If the compound contains hydrogen also, knock-on protons produce the following reactions:

- (7)  $O^{16}(p,\gamma)F^{17} + 0.59 \text{ Mev: } F^{17} \xrightarrow[70 \text{ s}]{\beta^+} O^{17}$
- (8)  $O^{18}(p,\alpha)N^{15} + 3.97 \text{ Mev: } N^{15} \text{ is stable}$
- (9)  $O^{18}(p,n)F^{18} - 2.45 \text{ Mev: } F^{18} \xrightarrow[112 \text{ m}]{\beta^+} O^{18}$

Of the nine reactions listed above, the third, fifth, and sixth result in the emission of penetrating radiation, and, therefore, need to be considered in the design of shielding for the external part of the cooling system when the coolant contains oxygen. In addition, there will be annihilation gamma-rays caused by the positrons emitted in the second, seventh, and ninth reactions. The energy listed for each reaction is the Q value for that reaction. The significance of Q will be discussed later.

Radioactive isotopes that will be produced in coolants containing oxygen are listed since 95% of all present day nuclear reactors use coolants which contain oxygen.<sup>1,2</sup> These radioactive isotopes will be produced regardless of how pure the coolant may be.

---

<sup>1</sup>Directory of Nuclear Reactors, Vol. I: Power Reactors (Kärntner Ring, Vienna 1, Austria: The International Atomic Energy Agency, 1959).

<sup>2</sup>Directory of Nuclear Reactors, Vol. II: Research, Test, and Experimental Reactors (Kärntner Ring, Vienna 1, Austria: The International Atomic Energy Agency, 1959).

The Importance of Water-Cooled Nuclear Reactors

TABLE I shows the importance of water-cooled nuclear reactors.<sup>1,2</sup> Over 59% of all nuclear reactors are water cooled and 74% of all research, test, and experimental reactors are water cooled. Of even greater significance is the fact that 76% of all nuclear reactors; 52% of all power reactors; and 90% of all research, test, and experimental reactors are liquid cooled.

The maximum thermal neutron flux in a continuously operating nuclear reactor ( $6.2 \times 10^{14}$  neutrons per square centimeter per second) occurs in a water-cooled research reactor.

---

<sup>1</sup>Directory of Nuclear Reactors, Vol. I: Power Reactors (Kärntner Ring, Vienna 1, Austria: The International Atomic Energy Agency, 1959).

<sup>2</sup>Directory of Nuclear Reactors, Vol. II: Research, Test, and Experimental Reactors (Kärntner Ring, Vienna 1, Austria: The International Atomic Energy Agency, 1959).

TABLE I  
NUCLEAR REACTOR COOLANTS

125 Nuclear Reactors			
94 Liquid Cooled (73 Water Cooled)			
29 Gas Cooled			
117 Coolants Containing Oxygen			
94 Coolants Containing Oxygen and Hydrogen			
48 Power Reactors		77 Research, Test, and Experimental Reactors	
25 Liquid Cooled	23 Gas Cooled	69 Liquid Cooled	6 Gas Cooled
16 Water Cooled		57 Water Cooled	
42 Coolants Containing Oxygen		75 Coolants Containing Oxygen	
20 Coolants Containing Oxygen and Hydrogen		74 Coolants Containing Oxygen and Hydrogen	

## CHAPTER II

### DESCRIPTION OF EXPERIMENTAL FACILITIES

Ideally, the type of nuclear reactor chosen for the experimental work should be the most representative of nuclear reactor cooling systems in general. As we have seen, a water-cooled nuclear reactor is the most representative. In addition, it is probably the simplest system to study. Finally, a water-cooled nuclear reactor with a significant neutron flux was available for experimentation.

#### General Description of the Oak Ridge National Laboratory Research Reactor

The nuclear reactor chosen for the basis of the experimental work was the Oak Ridge National Laboratory Research Reactor (ORR) at Oak Ridge, Tennessee. The design of the ORR incorporates a heterogeneous core which utilizes enriched uranium fuel with ordinary water as coolant and moderator.<sup>1</sup> The reflector is a relatively thin layer (3 to 6 inches) of beryllium metal, backed by a thick layer (approximately 4 feet) of water.

TABLE II lists the more important characteristics of the ORR that are pertinent to the following discussion. The quantities  $v$ ,  $b$ ,  $c$ ,  $G$ ,  $t$ , and  $t_R$  will be defined here and will be discussed more fully later.  $v$  is the volume of the cooling system in milliliters.  $b$  is the flow rate through the demineralizers in milliliters per second divided by  $v$ .  $c$  is

---

<sup>1</sup>T. E. Cole and J. P. Gill, The Oak Ridge National Laboratory Research Reactor (ORR) - A General Description, Oak Ridge National Laboratory Report Number 2240, (Oak Ridge, Tennessee: January 21, 1957).

TABLE II

CHARACTERISTICS OF THE OAK RIDGE NATIONAL  
LABORATORY RESEARCH REACTOR

$$v = 2.48 \times 10^8 \text{ milliliters}$$

$$b = 2.07 \times 10^{-5} \text{ reciprocal seconds}$$

$$c = 6.36 \times 10^{-7} \text{ reciprocal seconds}$$

$$G = 1.27 \times 10^{-5} \text{ reciprocal seconds}$$

$$\text{Average thermal neutron flux} = 1.8 \times 10^{14} \text{ neutrons per square centimeter per second}$$

$$\text{Maximum thermal neutron flux} = 5.4 \times 10^{14} \text{ neutrons per square centimeter per second}$$

$$\text{Average fast neutron flux} = 5.4 \times 10^{14} \text{ neutrons per square centimeter per second}$$

$$\text{Average fission neutron flux} = 2.59 \times 10^{14} \text{ neutrons per square centimeter per second}$$

$$t = 2.19 \times 10^2 \text{ seconds}$$

$$\text{Area} = 4.05 \times 10^5 \text{ square centimeters (area of aluminum in the reactor core)}$$

$$t_R = 5.94 \times 10^{-2} \text{ seconds}$$

$$\text{Power} = 30 \times 10^6 \text{ watts}$$

the make-up flow rate<sup>1</sup> in milliliters per second divided by  $v$ .  $G$  is the flow rate through the vacuum degasifier in milliliters per second divided by  $v$ .  $t$  is the time required to complete one cycle in seconds.  $t_R$  is the average retention time of the cooling water in the reactor core in seconds obtained by dividing the fluid volume of the core by the average volume flow rate of the coolant through the core.

Illustration 1 is a schematic diagram of the ORR cooling system. The filters and strainers shown remove a negligible amount of the radioactive isotopes from the coolant. Experimental data justifying this statement is given later. Illustration 2 shows how the water moves around and through the core. Illustration 3 is a more detailed drawing of the reactor core.

#### Ion Exchange System of the ORR

The demineralizer system, consisting of cation and anion "pre-columns" preceding a mixed bed column, was developed at the Oak Ridge National Laboratory (ORNL). The ion exchangers can be operated at high flow rates, up to 10 gallons per minute per cubic foot of resin, and still remove most of the radioactivity from the water. Each cation resin column contains 30 cubic feet of Amberlite IR-120 resin, and each anion resin column contains 26 cubic feet of IRA-401 resin. Each mixed-bed resin column contains 12 cubic feet of IR-120 and 18 cubic feet of IRA-401 resin. Ordinarily the flow rate through one of the demineralizer systems is 80 gallons per minute. There are two complete demineralizer systems, only

---

<sup>1</sup>The make-up flow rate is simply the amount of dilution water added to the reactor cooling system. Naturally, an equal amount is bled off elsewhere in the cooling system.

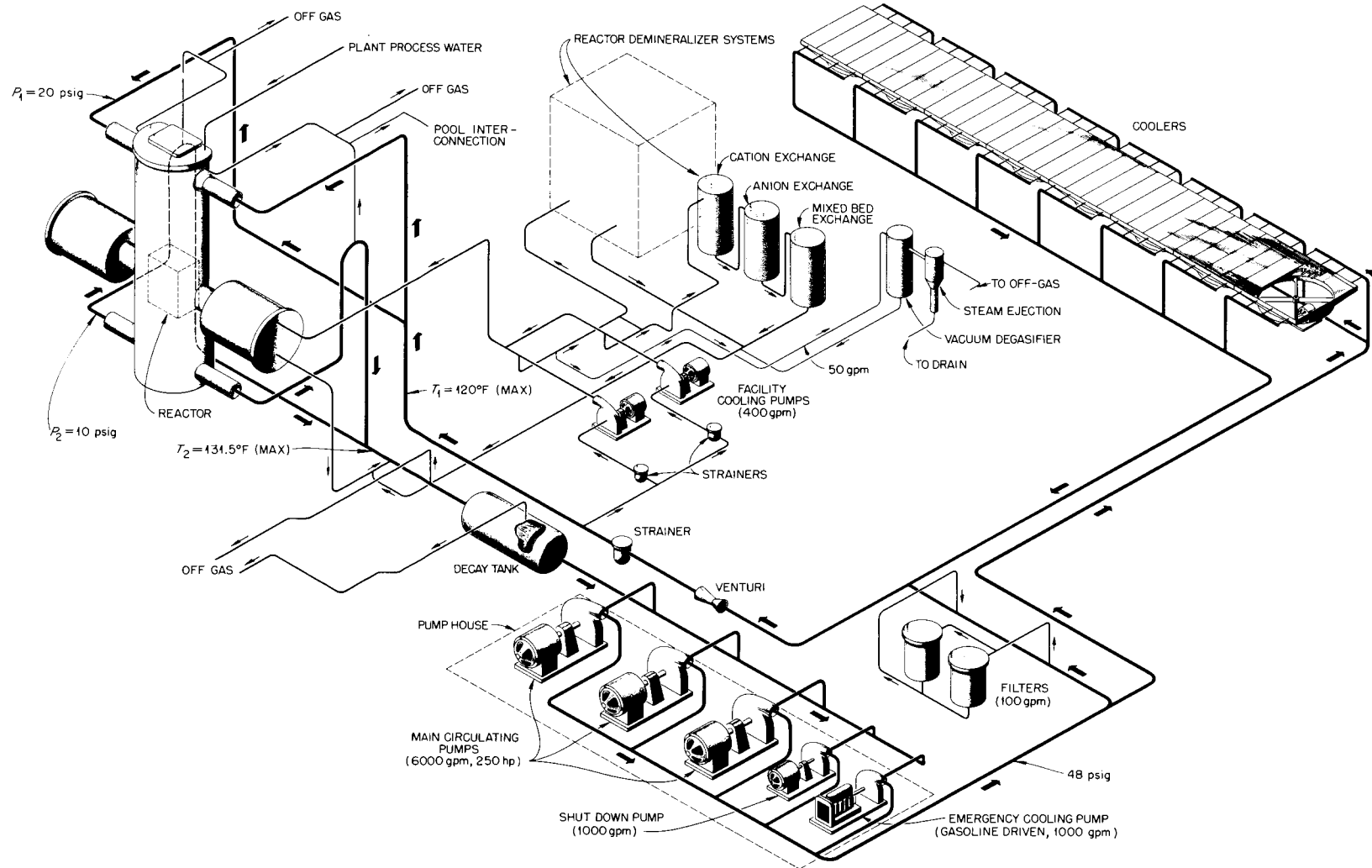


Illustration 1. - REACTOR COOLING SYSTEM

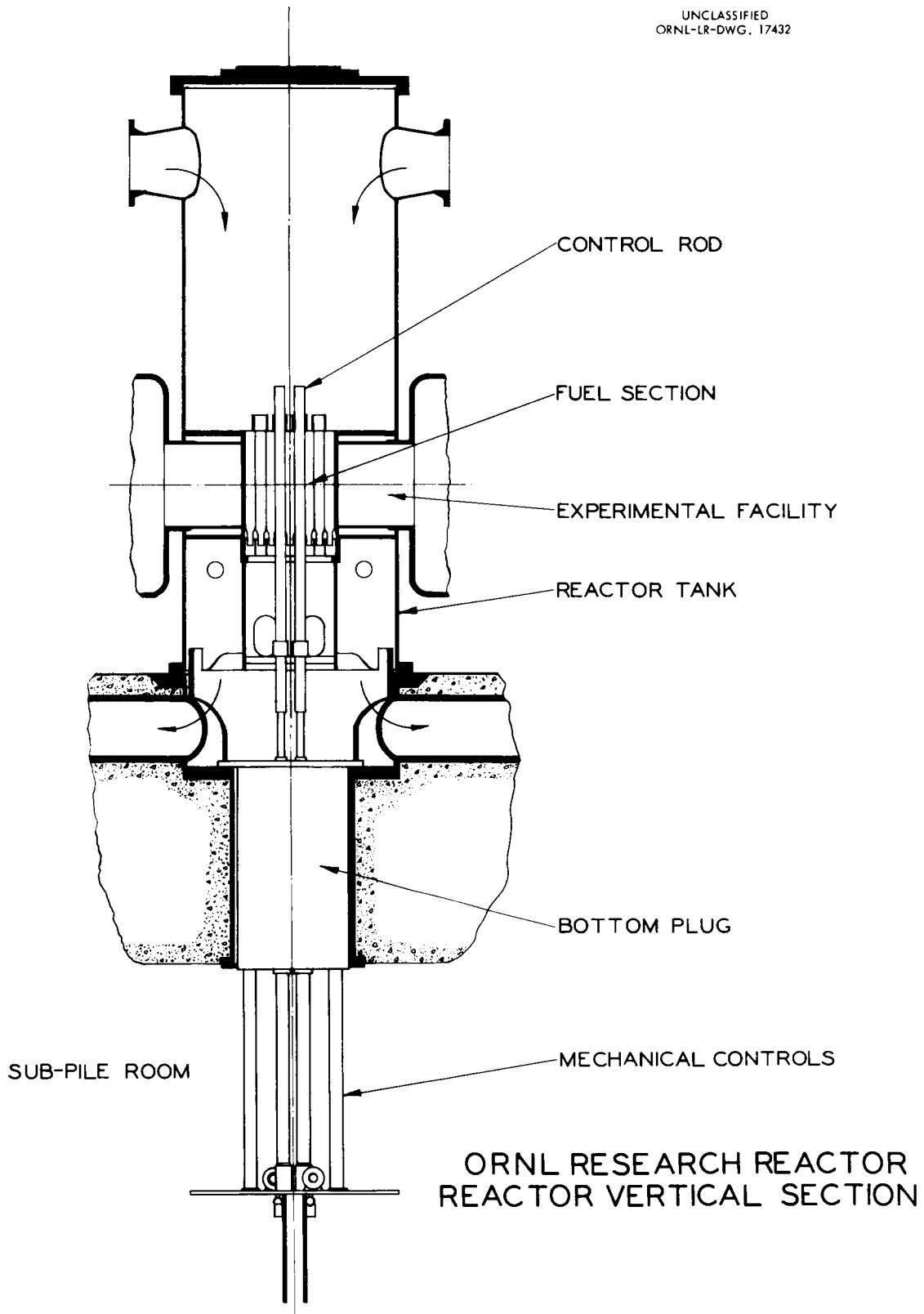
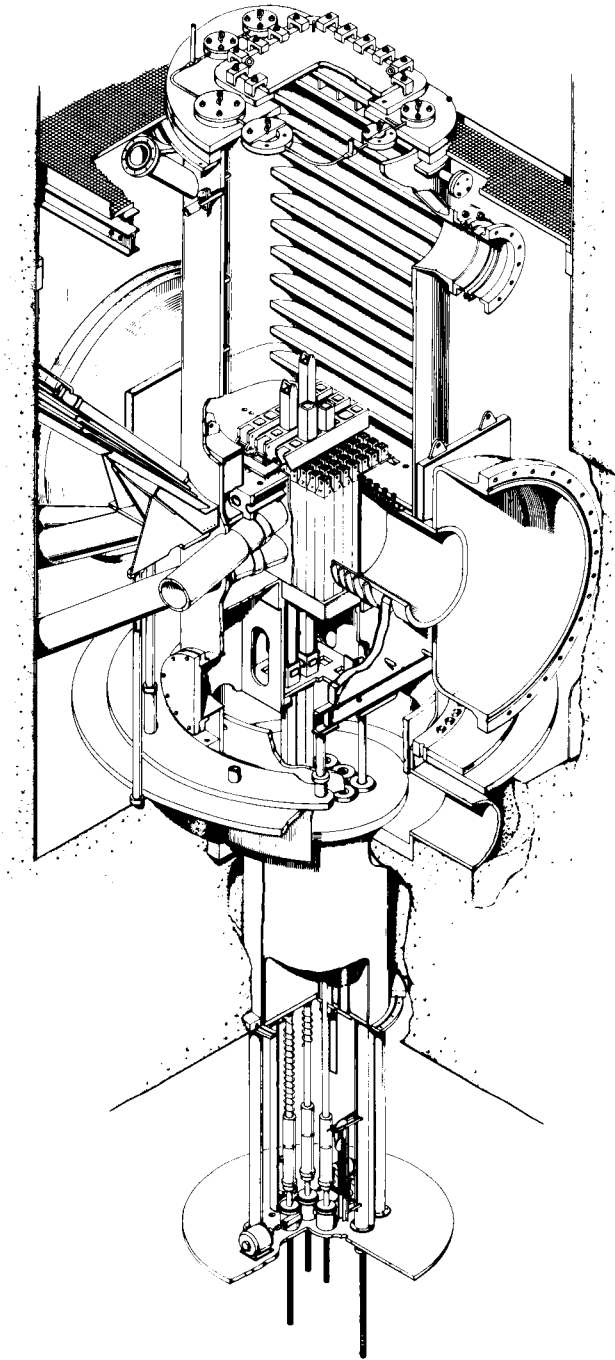


Illustration 2



OAK RIDGE RESEARCH REACTOR  
OAK RIDGE NATIONAL LABORATORY

Illustration 3

one of which is used at a time while the other system is kept in reserve.

## CHAPTER III

### EXPERIMENTAL RESULTS

All of the experimental results were obtained with the reactor at full power (30 megawatts).

#### A Method for the Analysis of Dissolved Gases in Water

In the analysis of the demineralized make-up water, it became evident that a method was needed whereby water could be analyzed for dissolved gases in the same manner as for dissolved solids.

Neutron activation analysis was obviously the method of choice.<sup>1</sup> The reason for this choice is that any dissolved gas or dissolved solid that would contribute to the activity of the cooling water would also show up in a neutron activation analysis.

In a neutron activation analysis, the elements present usually are identified by their respective gamma-ray energies and half-life. For quantitative determinations, two samples are used. One sample contains the water to be analyzed and the other sample contains demineralized water with a known concentration of the substance in question. After simultaneous irradiation in the same neutron flux, the activity of the unknown times the concentration of the standard divided by the activity of the standard equals the concentration of the unknown.

---

<sup>1</sup>C. E. Crouthamel, Applied Gamma-Ray Spectrometry (New York: Pergamon Press, 1960).

The difficulty with activation analysis of dissolved gases is that the concentration in the standard is difficult to determine. The method proposed here involves bubbling the desired gas through the standard water solution until the water is saturated with this gas. After this is completed, the standard is sealed and the concentration is determined from the temperature of the solution.

In order to ascertain the concentration of a gas in a solution as a function of temperature, reference must be made to standard works on the subject.<sup>1</sup> Usually the value of Henry's Law Constant  $K$  in millimeters of mercury per mole fraction is tabulated as a function of absolute temperature  $T_a$  in degrees Kelvin. Now<sup>2</sup>

$$K = \frac{P_A}{N_A} \quad (1)$$

where

$P_A$  is the partial pressure of the solute in millimeters of mercury ( $P_A = 760$  millimeters of mercury at one atmosphere pressure), and

$N_A$  is the mole fraction of the solute in the solution. And

$$N_A = \frac{n_A}{n_A + n_B} \quad (2)$$

where

$n_A$  is the number of moles of the solute, and

$n_B$  is the number of moles of the solvent. In addition,

<sup>1</sup>Edward W. Washburn and others, International Critical Tables, Vol. III, (New York: McGraw-Hill Book Company, 1928), p. 255.

<sup>2</sup>Farrington Daniels and Robert A. Alberty, Physical Chemistry (New York: John Wiley and Sons, Inc., 1958).

$$n_A = \frac{w_A}{M_A} \text{ and } n_B = \frac{w_B}{M_B} \quad (3)$$

where

$w_A$  is the weight of the solute A in grams,

$M_A$  is the molecular weight of the solute A in grams per mole,

$w_B$  is the weight of the solvent B in grams, and

$M_B$  is the molecular weight of the solvent B in grams per mole.

By combining equations (1), (2), and (3) and solving for  $w_A/w_B$ , one obtains

$$\frac{w_A}{w_B} = \frac{P_A M_A}{M_B (K - P_A)} \quad (4)$$

Finally,

$$p = \left( \frac{w_A}{w_B} \right) (10^6) = \frac{P_A (10^6) M_A}{M_B (K - P_A)} \quad (5)$$

where

$p$  is the concentration of the solute in the solvent in parts per million (ppm).

The variation of  $K$  with temperature is known to be<sup>1</sup>

$$\log_{10} K = \frac{0.05223(-D)}{T_a} + B \quad (6)$$

where

$D$  is the partial latent heat of vaporization of the gas from the solution in joules per gram-mole (the heat absorbed when one gram-mole of the gas is vaporized reversibly from an infinite amount of the solution), and

$B$  is a constant for any specific solvent and solute.

---

<sup>1</sup>Edward W. Washburn and others, International Critical Tables, Vol. III, New York: McGraw-Hill Book Company, 1928), p. 255.

Hence, if the value of  $K$  is known at any two different temperatures, or if the values of  $K$  and  $D$  are known at any one temperature ( $D$  and  $B$  are independent of temperature), then the value of  $K$  can be determined for any temperature (short of the boiling point of the solvent). If the absolute atmospheric pressure is different from 760 millimeters of mercury, then this value of  $P_A$  should be used in the calculations. The constant 0.05223 in equation (6) contains the value of the molar gas constant.

In practice the values of  $K$  may depart somewhat from the values predicted by equation (6), so one should use two values of  $K$  as close to the desired temperature as possible. The standard used in the activation analysis for argon reported herein was prepared in this manner.

#### Analysis of the Demineralized

##### Make-Up Water

In order to obtain a qualitative idea of the impurities in fresh demineralized make-up water, samples of it were irradiated in position number 2 of hole 71 of the Oak Ridge National Laboratory Graphite Reactor for periods of 10 minutes, 16 hours, and one week.<sup>1</sup> The only radioactive isotopes observed were  $\text{Na}^{24}$  and  $\text{A}^{41}$ . A comparative neutron activation quantitative analysis made by the author showed that there was  $0.396 \pm 0.003$  ppm sodium and  $0.599 \pm 0.006$  ppm argon in the demineralized make-up water at  $20^\circ\text{C}$ .

---

<sup>1</sup>The thermal neutron flux in this position was determined to be  $7.58 \times 10^{11}$  neutrons per square centimeter per second and the fission neutron flux was determined to be  $4.03 \times 10^9$  neutrons per square centimeter per second. The fluxes were determined by the author by irradiating sodium carbonate and cadmium covered aluminum. The neutron reactions used in these determinations were  $\text{Na}^{23}(n,\gamma)\text{Na}^{24}$  and  $\text{Al}^{27}(n,\alpha)\text{Na}^{24}$ . The respective cross-sections for these neutron reactions are 0.525 barns and 0.600 millibarns. In each case, the activity of  $\text{Na}^{24}$  was measured.

Concentration of Stable Elements in  
the Cooling Water

A quantitative neutron activation analysis of the cooling water yielded the results tabulated in TABLE III. The value listed for oxygen is a calculated value that will be convenient in later calculations. The value listed for  $U^{235}$  is inferred from the results of discussion that follows later on. No analysis was made for argon since its concentration is rapidly reduced after start up by the vacuum degasifier. Also, the equilibrium concentration of argon would be dependent on the temperature of the demineralized make-up water and the atmospheric pressure.

The concentration of sodium is apparently reduced by the reactor demineralizers. The cause of this change is unknown. However, aluminum and cadmium are found in the reactor cooling water which indicates that relatively large areas of these elements are exposed to the reactor cooling water.

Method of Analysis of Cooling Water  
for Radioactive Isotopes

Gamma scintillation spectrometry<sup>1</sup> was used in the analysis of the cooling water for gamma-ray emitters. The analyzer used had a built-in automatic dead-time correction mechanism.<sup>2</sup> It also had an add-subtract

---

<sup>1</sup>C. E. Crouthamel, Applied Gamma-Ray Spectrometry (New York: Pergamon Press, 1960).

<sup>2</sup>For the sake of accuracy, the dead-time was kept below 40% in all cases. The dead-time was read directly on a dial with a range of 0 to 100%. The analyzer had 200 channels and was manufactured by Radiation Instrument Development Laboratory, Incorporated, Northlake, Illinois.

TABLE III  
CHEMICAL COMPOSITION OF THE  
ORR COOLING WATER

Element	Concentration in Parts per Billion (ppb)
O	$8.90 \times 10^8$
Na	$5.46 \pm 0.04$
Mg	$\leq (531 \pm 16)$
Al	$8.80 \pm 0.84$
Zn	$\ll 100$
Cd	$14.3 \pm 0.1$
$U^{235}$	$\ll 33.7 \times 10^{-3}$

logic, that is, the ability to subtract data being fed in from data already on the analyzer memory. The readout mechanism printed the channel number versus the number of counts collected in that channel, thus, reducing the possibility of error. A visible oscilloscope readout of the data in the memory functioned even while the analyzer was counting.

A thallium-activated sodium iodide crystal cylinder, 3 inches in diameter and 3 inches tall served as the scintillator used in the scintillation counter to obtain all the measurements reported here. In the analysis of complex spectra, it would be ideal to suppress the Compton electron distribution completely. However, to go to a larger phosphor would require the use of a larger phototube or a set of smaller phototubes with an appreciable increase in cost and loss of resolution. The crystal was magnetically shielded. The sampling point was a tap into one of the main exit water pipes from the reactor. This made it possible to count the water a very few seconds after it left the reactor core. Although the sampling point is just slightly downstream from one of the off-gas lines, this does not effect the results since a very sensitive rotameter on the off-gas line indicated no flow whatever through it.

Design of the Apparatus Used to Study Short  
Half-Life Radioactive Isotopes  
in the Cooling Water

Here a 10 milliliter counting volume was obtained by coiling a suitable length of 3/16 inch (internal diameter) tygon tubing inside of a 3 inch diameter glass sphere. A polystyrene absorber 2 inches thick and 3 inches in diameter was placed directly on top of the sodium iodide

crystal. Polystyrene is a very good material for this purpose since the bremsstrahlung will be much less than for a material such as aluminum or lead because the quantity of bremsstrahlung produced by the beta radiations is directly proportional to the atomic number  $Z$  of the absorber, all other quantities being constant.<sup>1</sup>

The required thickness of the polystyrene absorber to minimize bremsstrahlung was calculated by using the relation<sup>2</sup>

$$R_{\beta} = 0.571 E_{\beta} - 0.161 \quad (7)$$

where

$R_{\beta}$  is the range of the beta particle in grams per square centimeter, and  $E_{\beta}$  is the energy of the beta particle in Mev.

Since  $N^{16}$  has the most energetic beta radiation energy (10.0 Mev), this was used as the basis for the absorber thickness determination.<sup>3</sup> Polystyrene has a density of 1.16 grams per cubic centimeter, and actually only 4.78 centimeters of absorber were required; however, for convenience, 5.08 centimeters were used.

The glass sphere rested directly on top of the absorbers, and the whole apparatus was shielded by 4 inches of lead. The lead shield was large enough so that backscatter was negligible.<sup>4</sup> The lead shield was lined on the inside with 0.036 inches of cadmium (99.9% pure) and 0.016

<sup>1</sup>Robley D. Evans, The Atomic Nucleus (New York: McGraw-Hill Book Company, Inc., 1955).

<sup>2</sup>Ernst Bleuler and George J. Goldsmith, Experimental Nucleonics (New York: Rinehart and Company, Inc., 1956).

<sup>3</sup>James M. Cork, Radioactivity and Nuclear Physics (New York: D. Van Nostrand Company, Inc., 1957).

<sup>4</sup>The lead shield was 8 x 8 x 18 inches.

inches of copper inside of the cadmium. The cadmium liner greatly reduces the effect of lead x-ray production in the lead shield.

By varying the flow rate of the cooling water through the counting volume, the half-lives of the various short half-life gamma-ray energy peaks could be determined. Corrections were made for absorption of the gamma rays in the water, tygon hose, glass, and absorbers. In addition, corrections were made for decay while the coolant was passing through the counting volume.

Method of Analysis of the Cooling Water for Long  
Half-Life Radioactive Isotopes  
in the Cooling Water

Since some of the activities were too low to be detected in the arrangement just described, a more sensitive device was utilized for the detection of these latter radioactive isotopes. Here a counting volume of 3000 milliliters was used that surrounded the crystal on all sides except the bottom where the photomultiplier tube was connected. By making measurements at intervals of time, all the radioactive isotopes were identified by both gamma-ray energy and half-life. In computing specific activities, corrections were made for absorption of the gamma-rays in the water and the walls of the containing vessel. The lead shield used was, for all practical purposes, identical to the shield previously described.

Measured Concentrations of Radioactive  
Isotopes in the Cooling Water

Determination of Disintegration Rate  
From Spectral Data

The disintegration rate of a radioactive isotope is given by the following relationship.<sup>1</sup>

$$N_{\gamma} = \frac{C}{\epsilon P I F} \quad (8)$$

where

$N_{\gamma}$  is the number of disintegrations per second,

C is the area under the photo-peak in counts per second,

$\epsilon$  is the total absolute detection efficiency for the source-detector geometry used,

P is the appropriate value for the peak-to-total ratio (P is the ratio of C to the total area of the gamma-ray spectrum),

I is a correction factor either for absorption of gamma radiations in the source and/or any beta absorber used in the measurement, and

F is the number of gamma-rays of this energy emitted per disintegration expressed as a decimal fraction. The value of F can be determined from any one of a number of sources.<sup>2,3,4,5</sup>

The value of I can be obtained from the following relationship:

<sup>1</sup>R. L. Heath, Scintillation Spectrometry Gamma-Ray Spectrum Catalogue, Phillips Petroleum Co. Report Number IDO-16408, (Idaho Falls, Idaho: July 1, 1957).

<sup>2</sup>C. E. Crouthamel, Applied Gamma-Ray Spectrometry (New York: Pergamon Press, 1960).

<sup>3</sup>D. Strominger, J. M. Hollander, and G. T. Seaborg, "Table of Isotopes," Reviews of Modern Physics, XXX, Part II (April, 1958), pp. 585-904.

<sup>4</sup>Simon Kinsman and others, Radiological Health Handbook (Cincinnati, Ohio: Robert A. Taft Sanitary Engineering Center, 1957).

<sup>5</sup>"Nuclei Formed in Fission: Decay Characteristics, Fission Yields, and Chain Relationships," Journal of the American Chemical Society, LXVIII (1946), pp. 2411-2442.

$$I = e^{-\mu \rho x} \quad (9)$$

where

$\mu$  is the coefficient of absorption in square centimeters per gram,  $\rho$  is the density of the absorber in grams per cubic centimeter, and  $x$  is the thickness of the absorber in centimeters.

The Peak-to-Total Ratio as a Function  
of Gamma-Ray Energy

Heath<sup>1</sup> tabulates experimental values of P for gamma-ray energies of 0.155, 0.323, 0.478, 0.662, 0.835, 1.114, 1.29, 1.78, 1.83, 2.76, and 3.13 Mev. The error is estimated to be less than  $\pm 2\%$  for all measurements. The values of P were given for sodium iodide detectors 3 inches in diameter by 3 in. thick at a distance of 10 centimeters from the source. Since the value of P has a negligible variation between 0.2 and 10 centimeters, these values may be used for other than distances of 10 centimeters.

From Heath's data, two empirical equations have been obtained which express P as a function of  $E_\gamma$ , the gamma-ray energy in Mev. For  $E_\gamma \leq 0.478$  Mev,

$$P = \exp \left[ -0.924 - 0.878 \ln E_\gamma - 0.216 (\ln E_\gamma)^2 \right] \quad (10)$$

and for  $E_\gamma \geq 0.478$  Mev,

$$P = \frac{0.414}{E_\gamma^{0.676}} \quad (11)$$

Equation (11) has a coefficient of correlation of -0.980 which indicates a correlation within experimental error.

---

<sup>1</sup>R. L. Heath, Scintillation Spectrometry Gamma-Ray Spectrum Catalogue, Phillips Petroleum Co. Report Number IDO-16408, (Idaho Falls, Idaho: July 1, 1957).

## Determination of Unknown

## Absorber Thickness

In the use of the 3 liter counting volume, it was not possible to determine the absorber thickness directly. However, it was possible to determine the absorber thickness  $x$  indirectly while calibrating the container with a single radioactive isotope. The only requirement is that the radioactive isotope have two gamma-rays of sufficiently different energy so that the respective values of  $\mu$  are sufficiently different for accurate calculations.

In order to obtain an equation that will give the absorber thickness  $x$  directly, one can start with equation (9) and express it as

$$I_1 = e^{-\mu_1 \rho x} \quad \text{and} \quad I_2 = e^{-\mu_2 \rho x} \quad (12)$$

where the subscripts 1 and 2 denote the low and high energy gamma-rays, respectively. Also,

$$q = \frac{\epsilon_1}{\epsilon_2} = \text{constant.} \quad (13)$$

Now equation (8) may be written as

$$N_\gamma = \frac{LC_1}{\epsilon_1 P_1 I_1 F_1} = \frac{C_2}{\epsilon_2 P_2 I_2 F_2} \quad (14)$$

where

$L$  is the fraction of the total area under the low energy peak due to the spectrum of the low energy peak.

Then by combining equations (12), (13), and (14) and solving for  $x$ , one obtains

$$x = \frac{\ln\left(\frac{P_2 F_2 LC_1}{q C_2 P_1 F_1}\right)}{\rho (\mu_2 - \mu_1)}. \quad (15)$$

TABLE IV lists the values of the various parameters in equation (15) for  $\text{Na}^{24}$ . The constant L can be easily determined from a standard spectrum (no absorber) of the radioactive isotope used by using equations (13) and (14). Even though  $\epsilon$  varies greatly with distance from the crystal, the ratio of  $\epsilon_1$  to  $\epsilon_2$  is almost completely independent of distance. The value of x for the 3 liter counting volume turned out to be 0.754 centimeters and the value of x for the 10 milliliter counting volume was 5.08 centimeters.

Correction for Decay Within the Counting Volume  
for Continuous Flow Measurements

The advantage of using continuous flow for the measurement of short half-life activities is that the counting rate remains substantially constant. On the other hand, there is decay while the activity is passing through the counting volume. If the activity has decayed for  $T_1$  seconds before entering the counting volume and for  $T_2$  seconds at the time it leaves the counting volume, then the measured activity can be assumed to have decayed for  $T^*$  seconds which is given by the following equation:<sup>1</sup>

$$T^* = T_1 - \frac{1}{\lambda} \ln \left( \frac{1 - e^{-\lambda(T_2 - T_1)}}{\lambda(T_2 - T_1)} \right) \quad (16)$$

where

$T^*$  is the effective mean decay time at which measurements are made, and  $\lambda$  is the radioactive decay constant in reciprocal seconds.<sup>2</sup>

---

<sup>1</sup>Ernst Bleuler and George J. Goldsmith, Experimental Nucleonics (New York: Rinehart and Company, Inc., 1956).

<sup>2</sup>Throughout this work, the value of  $\lambda$  for the parent is used where the half-life of the parent is greater than that of the daughter.

TABLE IV

VALUES FOR THE DETERMINATION OF ABSORBER  
THICKNESS WITH  $\text{Na}^{24}$ 

$$L = 0.923$$

$$q = 1.19$$

$$F_1 = F_2 = 1.00$$

$$P_1 = 0.333$$

$$P_2 = 0.214$$

$$\left. \begin{array}{l} \mu_1 = 0.0600 \text{ square centimeters per gram} \\ \mu_2 = 0.0413 \text{ square centimeters per gram} \end{array} \right\} \text{ for water}$$

$$E_{\gamma 1} = 1.368 \text{ Mev}$$

$$E_{\gamma 2} = 2.754 \text{ Mev}$$

$$\rho = 1.00 \text{ gram per cubic centimeter for water}$$

In the case of the 10 milliliter counting volume, the volume of the line leading from the tap on the exit cooling water line to the counting container was 195 milliliters. For the determination of  $N^{17}$  this volume was 171 milliliters.

#### Fundamental Data Used

In interpretation of experimental results of this kind, it is necessary to use data in the literature that might conceivably change slightly in the future. Thus, in an effort to prevent the experimental results from being dated, the fundamental information used in the calculations will be given.

All of the peak-to-total ratios were computed on the basis of equations (10) and (11). TABLE V lists the fundamental data used in the calculations. Under the half-life column, the abbreviations S, M, H, and D stand for seconds, minutes, hours, and days respectively. Since  $\text{La}^{140}$  exhibited the half-life of its parent  $\text{Ba}^{140}$ , and  $\text{In}^{115\text{m}}$  exhibited the half-life of its parent  $\text{Cd}^{115}$ , the parent half-lives are the ones actually used in the calculations.<sup>1</sup> The photon energies listed are the peaks on which the quantitative results are based. The value of F for  $N^{17}$  means that it was assumed that one neutron was emitted per disintegration. The value of F for  $\text{Cd}^{115}$  was determined in this study by assuming equilibrium between  $\text{Cd}^{115}$  and its daughter  $\text{In}^{115\text{m}}$ . The relative activities are<sup>2</sup>

$$\frac{N_{\gamma 1}}{N_{\gamma 2}} = \frac{\lambda_2 - \lambda_1}{\lambda_2} \quad (17)$$

<sup>1</sup>A daughter radioactive isotope exhibits the half-life of its parent when the parent half-life is longer and the two are at equilibrium.

<sup>2</sup>Ernst Bleuler and George J. Goldsmith, Experimental Nucleonics (New York: Rinehart and Company, Inc., 1956).

TABLE V  
FUNDAMENTAL DATA USED

Nuclide	Half-Life	Photon Energy in Mev	F	€ at 6.16 Centimeters	€ at 8.48 Centimeters	μ in Square Centimeters per Gram (for water)
${}^7\text{N}^{16}$	7.35 S	6.13	0.550		0.0170	0.0275
${}^7\text{N}^{17}$	4.14 S		1.00			
${}^8\text{O}^{19}$	29.4 S	0.200	0.300		0.0385	0.136
${}^{11}\text{Na}^{24}$	15.0 H	2.754	1.00		0.0180	0.0413
${}^{12}\text{Mg}^{27}$	9.45 M	0.834	0.700		0.0246	0.0769
${}^{13}\text{Al}^{28}$	2.27 M	1.78	1.00		0.0198	0.0524
${}^{30}\text{Zn}^{65}$	245 D	1.12	0.460	0.0353		0.0668
${}^{48}\text{Ca}^{115\text{m}}$	43.0 D	0.940	< 0.0200	0.0375		0.0724
${}^{48}\text{Ca}^{115}$	2.20 D	0.520	(0.748)	0.0457		0.0953
${}^{49}\text{In}^{115\text{m}}$	4.50 H	0.335	0.950	0.0526		0.113
${}^{56}\text{Ba}^{140}$	12.8 D					
${}^{57}\text{La}^{140}$	40.2 H	1.60	0.740	0.0321		0.0553

where

the subscript 1 denotes the parent, and the subscript 2 denotes the daughter. The activity of  $\text{Ba}^{140}$  was calculated from the activity of  $\text{La}^{140}$  by equation (17). The  $\epsilon$  values at 6.16 centimeters were applied to the counting volume of 3 liters and the  $\epsilon$  values at 8.48 centimeters were applied to the counting volume of 10 milliliters. It was found experimentally that the value of  $\mu$  for water applied also to polystyrene with negligible error.

### Experimental Results

TABLE VI tabulates the experimental results. The decay time before counting is based on the fact that it takes 6.24 seconds for the water to go from the reactor core exit to the tap at a flow rate of 17,900 gallons per minute through the core. This flow rate fluctuates approximately  $\pm 1\%$ . The decay times listed in TABLE VI are the times that elapsed before the gamma-ray peak was evaluated. The variation in decay time was necessary in order that the photopeaks of the shorter half-life radioactive isotopes would be decayed away where these photopeaks overlapped the gamma-ray peaks of the longer half-life radioactive isotopes. Of course, all the results listed are corrected for the decay time and are the maximum activities in the cooling system immediately after passing through the core at the time they were taken.  $a$  is the equilibrium specific activity of a radioactive isotope in disintegrations per second per milliliter of reactor cooling water.<sup>1</sup>  $a_n$  is the specific activity at  $n$  cycles. The values

---

<sup>1</sup>The equilibrium specific activity,  $a$ , in this dissertation will be understood to mean the maximum specific activity of the coolant for any one cycle at equilibrium. It is assumed that this maximum specific activity is attained immediately after leaving the reactor core.

TABLE VI

CONCENTRATION OF RADIOACTIVE ISOTOPES  
IN THE COOLING WATER

Nuclide	Decay Time Before Counting	n in Cycles	$a_n$ in Disintegrations per Second per Milliliter of Cooling Water at n Cycles	a in Disintegrations per Second per Milliliter of Cooling Water at Equilibrium ( $n = \infty$ )
${}^7\text{N}^{16}$	24.5 S	307	$6.50 \times 10^5$	$6.50 \times 10^5$
${}^7\text{N}^{17}$	17.3 S		$5.38 \times 10^2$	$5.38 \times 10^2$
${}^{80}\text{O}^{19}$	81.5 S	307	$6.90 \times 10^4$	$6.90 \times 10^4$
${}^{11}\text{Na}^{24}$	20.3 H	307	$9.66 \times 10^2$	$1.07 \times 10^3$
${}^{12}\text{Mg}^{27}$	5.92 M	307	$2.90 \times 10^3$	$2.90 \times 10^3$
${}^{13}\text{Al}^{28}$	1.36 M	307	$2.38 \times 10^3$	$2.39 \times 10^3$
${}^{30}\text{Zn}^{65}$	12.1 D	701	$7.87 \times 10^{-1}$	3.17
${}^{48}\text{Cd}^{115\text{m}}$	8.00 D	701	$> 1.45 \times 10$	$> 5.26 \times 10$
${}^{48}\text{Cd}^{115}$	7.00 D	701	$9.64 \times 10$	$3.10 \times 10^2$
${}^{49}\text{In}^{115\text{m}}$	7.00 D	701	$1.05 \times 10^2$	$3.45 \times 10^2$
${}^{56}\text{Ba}^{140}$	192 H	701	$2.76 \times 10^{-1}$	1.65
${}^{57}\text{La}^{140}$	192 H	701	$3.16 \times 10^{-1}$	1.89

of  $a_n$  were determined using the numerical values given in TABLE V and elsewhere and equations (8), (9), (10), (11), (15), (16), and (17).  $\text{Na}^{24}$  was measured in both counting volumes. Since the number of cycles between the two sets of measurements was known, by assuming that the initial activity of  $\text{Na}^{24}$  was zero, it was possible to calculate the effective number of cycles in both cases by methods which will be discussed later. It was also assumed that the initial activity of all the other radioactive isotopes was zero at  $n = 0$  which is a good assumption since the entire cooling system had been drained and refilled prior to these experiments. The value of  $n$  for  $\text{N}^{17}$  is not needed since  $\text{N}^{17}$  builds up to its maximum activity in one cycle. The method of determining the activity of  $\text{N}^{17}$  will be explained later. The values of  $a$  were calculated by methods which will be discussed later using the numerical values listed in TABLE VI and the tabulated values of  $a_n$ .

TABLE VII lists the values of  $\Delta a$  and  $r$  for the various radioactive isotopes in the reactor cooling system.  $\Delta a$  is the change in the specific activity of the coolant at equilibrium on passing through the reactor core in disintegrations per second per milliliter of reactor cooling fluid.  $r$  is the rate of production of the radioactive isotope in the coolant in atoms per second. The methods of calculating  $\Delta a$  and  $r$  will be given later.  $\Delta a$  and  $r$  are the only significant quantities in a reactor cooling system since once they are determined they are independent of the flow rate through the demineralizers, the make-up water flow rate, the flow rate through the vacuum degasifier, and the efficiencies of ion exchange and degasification. Both quantities are directly proportional to the neutron flux and hence to the reactor power since the neutron flux is

TABLE VII  
 RATE OF PRODUCTION OF RADIOACTIVE ISOTOPES  
 IN THE COOLING WATER

Nuclide	$\Delta a$ in Disintegrations per Second per Milliliter	r in Atoms per Second
${}^7\text{N}^{16}$	$6.50 \times 10^5$	
${}^7\text{N}^{17}$	$5.38 \times 10^2$	
${}^{80}\text{O}^{19}$	$6.87 \times 10^4$	
${}^{11}\text{Na}^{24}$	8.00	$7.14 \times 10^{11}$
${}^{12}\text{Mg}^{27}$	$6.87 \times 10^2$	$7.31 \times 10^{11}$
${}^{13}\text{Al}^{28}$	$1.60 \times 10^3$	$5.93 \times 10^{11}$
${}^{30}\text{Zn}^{65}$	$1.27 \times 10^{-2}$	
${}^{48}\text{Cd}^{115\text{m}}$	$> 2.40 \times 10^{-1}$	$> 1.47 \times 10^{12}$
${}^{48}\text{Cd}^{115}$	1.65	$5.15 \times 10^{11}$
${}^{49}\text{In}^{115\text{m}}$	1.80	
${}^{56}\text{Ba}^{140}$	$4.35 \times 10^{-3}$	$7.89 \times 10^9$
${}^{57}\text{La}^{140}$	$5.00 \times 10^{-3}$	

directly proportional to the reactor power. Where the activities are due to recoil mechanism, then  $r$  is also independent of the flow rate through the reactor core, once it has been determined. Only the values of  $r$  are listed where the activity is probably produced by recoil mechanism. The values of  $r$  for  $\text{La}^{140}$  and  $\text{In}^{115\text{m}}$  are not listed since these are daughter products not produced directly by recoil mechanism. Since there is no zinc in the reactor core, the value of  $r$  for zinc is not listed.

### Measurement of $\text{N}^{17}$ in the Cooling Water

#### Development of a Liquid Neutron-Emitter

In order to determine the amount of  $\text{N}^{17}$  in the cooling water, it was first necessary to calibrate the counting equipment. For this reason, the development of a liquid neutron-emitter became necessary.

The first attempt involved using 6 milligrams of  ${}_{95}\text{Am}^{241}$  in combination with 171 milliliters of a saturated  $\text{Be}(\text{NO}_3)_2 \cdot 3\text{H}_2\text{O}$  aqueous solution.  $\text{Am}^{241}$  is an  $\alpha$ -emitter (5.534 Mev) with a specific activity of 3.17 curies per gram and a half-life of 458 years. Ordinarily  $\text{Am}^{241}$  when mixed with pure beryllium makes a very fine neutron source by means of the  $\text{Be}^9(\alpha, n)\text{C}^{12}$  reaction. However, no neutrons were detected, and it can only be concluded that the aqueous solution separated the  $\text{Be}^9$  and  $\text{Am}^{241}$  nuclei to such an extent that the  $\alpha$ -particles had insufficient energy to penetrate the intervening water layer and cause the desired reaction.

Since the  $(\gamma, n)$  threshold for beryllium is 1.67 Mev for the reaction  $\text{Be}^9(\gamma, n)\text{Be}^8$ ,  $\text{Na}^{24}$  was added to 171 milliliters of a fresh saturated aqueous beryllium nitrate solution with successful results. The yield was 2.27 neutrons per second per millicurie of  $\text{Na}^{24}$  per milliliter of

saturated aqueous beryllium nitrate solution. The resulting neutrons have an energy of 0.8 Mev.  $N^{17}$  emits a 0.9 Mev neutron. The liquid neutron-emitter was calibrated by comparison with a plutonium-beryllium source on the ORNL long counter. The long counter efficiency is approximately constant over the range of the neutron energies encountered.

#### Experimental Apparatus for the Detection of $N^{17}$

The neutrons were moderated with paraffin so that they would be detected by the neutron counters which are sensitive to thermal neutrons. The moderator tank was surrounded on the outside with a cadmium shield 0.036 inches thick which absorbed all but  $3.37 \times 10^{-5}$  per cent of the externally incident thermal neutrons. Four neutron detectors were equally spaced and located half way between the outside cadmium shield and the interior counting container. The detectors were the standard one-inch UG-59 B/U Amphenol 82-804 boron trifluoride neutron counters. The electronics used included a combination amplifier and pulse-height discriminator, scalar (with built-in timer), and high voltage chassis. The operating voltage was 2,100 volts.

The counting container used was a glass cold finger with a capacity of 171 cubic centimeters. This cold finger was inserted 7 inches into the center of the cylinder of paraffin and perpendicular to its base. The cylinder was 10 inches in diameter and 10 inches tall. The cold finger was approximately 1.25 inches in diameter. The four  $BF_3$  tubes were inserted 8.5 inches into the paraffin and parallel to the axis of the counting container. Holes in the paraffin for the  $BF_3$  tubes and the cold finger

were obtained by using several number 661 cellulose nitrate International Lusteroid centrifuge tubes.

The efficiency of the device for counting 0.8 Mev neutrons was  $1.34 \times 10^{-3}$ . The efficiency for counting  $\text{Na}^{24}$  disintegrations was  $1.12 \times 10^{-9}$ , so the counting rate due to gamma rays alone was negligible. The background counting rate was approximately 21 counts per minute with no neutron source present. The cause of this background is unknown.

By making measurements at different flow rates through the counting volume, the half-life of  $\text{N}^{17}$  against neutron emission ( $4.80 \pm 0.33$  seconds) was observed to approximately coincide with the published half-life of 4.14 seconds. Corrections were made for the decay of  $\text{N}^{17}$  while passing through the counting volume.

#### Argon

$\text{A}^{41}$  activity in the cooling water was not determined for several reasons. One reason for this omission is that the 1.29 Mev gamma-ray peak of  $\text{A}^{41}$  was covered by the 1.368 Mev peak of  $\text{Na}^{24}$ . Since the half-life of  $\text{A}^{41}$  is less than the half-life of  $\text{Na}^{24}$ , the gamma-ray peak of  $\text{A}^{41}$  will vanish before the gamma-ray peak of  $\text{Na}^{24}$ . Thus, waiting for the  $\text{Na}^{24}$  to decay out would be of no value.

The activity of  $\text{A}^{41}$  in the reactor cooling water decreases with time. This may be inferred from the results in TABLE VIII. These results were obtained with the 3-liter counting volume. The reason that the 1.83-hour  $\text{A}^{41}$  gamma-ray peak could be seen, even though the 15.0-hour  $\text{Na}^{24}$  peak usually covers it, was due to the cation exchanger removing almost all of

TABLE VIII  
DECREASE OF THE ACTIVITY OF A<sup>41</sup> WITH TIME

n in Cycles	Counts Per Minute of A <sup>41</sup>		
	Effluent From The Cation Exchanger	Effluent From The Anion Exchanger	Effluent From the Mixed-Bed Exchanger
43.9	1,280,000	468,000	206,000
236	166,000	105,000	133,000
641		36,600	68,800

the  $\text{Na}^{24}$ . Previously, it had been attempted to subtract out the  $\text{Na}^{24}$  peak, but the results were discouraging.

Although the results might indicate some removal of  $\text{A}^{41}$  by ion exchange, this really is immaterial.

The reason for the decrease in activity of  $\text{A}^{41}$  with time is that  $\text{A}^{41}$  is the only observed activity that is due only to an impurity of the stable element in the cooling water. This contention will be verified later. However, the amount of stable argon in the water decreases with time due to its removal by the vacuum degasifier, although it is added in slight amounts by the make-up water.

One might then argue that even though this is the case, an equilibrium value would still be reached. This idea is invalid since the amount of argon in the make-up water varies with the atmospheric pressure and the temperature of the make-up water, both of which vary somewhat, even during a period of one day.

Since the demineralized water is stored in an environment exposed to atmospheric air, one might be interested in calculating the amount of argon to be expected in such a water at equilibrium. This is easily done by first calculating the concentration of argon in the cooling water as if it were exposed to a pure argon atmosphere and had reached equilibrium (using the desired temperature and atmospheric pressure).

If this figure is multiplied by the decimal fraction of argon by volume in dry air at sea level (0.0094) times the quantity atmospheric pressure minus the vapor pressure of water at this temperature (since it must be assumed that the air in contact with the water is saturated with

water vapor) this gives the partial pressure of argon.<sup>1</sup> If this product is divided by the atmospheric pressure, the result is the concentration of argon in the water. The same procedure could be applied to other gases found in air. This procedure was applied to the demineralized water, and the calculated value of the concentration of argon in the demineralized water agreed with the experimental value within the experimental error shown.

If the vacuum degasifier was started early enough before the reactor was started, then it is obvious that the amount of  $A^{41}$  in the reactor cooling water would be very unlikely to be of any consequence compared with the various other activities present. Thus, the role of argon in the reactor cooling water appears to be unique.

#### Removal of Active Nuclides by Ion Exchange

One of the main assumptions that will be made in the theories to be developed is that the efficiency of ion exchange,  $E$ , expressed as a decimal fraction for the particular isotope in question, is a constant in time, and is independent of the activity of the radioactive isotope in question. Although this was subsequently verified in an indirect manner (which will be discussed later), it was also verified directly.

Only the radioactive isotopes  $Na^{24}$ ,  $Zn^{65}$ ,  $Cd^{115m}$ ,  $Cd^{115}$ ,  $In^{115m}$ ,  $Ba^{140}$ , and  $La^{140}$  were studied since ion exchange is a negligible factor<sup>2</sup> in the removal of the other radioactive isotopes previously discussed.

---

<sup>1</sup>Gordon Maskew Fair and John Charles Geyer, Water Supply and Waste-Water Disposal (New York: John Wiley and Sons, Inc., 1956).

<sup>2</sup>Their removal is by decay alone.

However, no results are listed for  $\text{Cd}^{115\text{m}}$  and  $\text{Ba}^{140}$  since their gamma-ray peaks were not observed. For purposes of calculation, the value of E for  $\text{Cd}^{115\text{m}}$  was assumed to be the same as the value of E for  $\text{Cd}^{115}$  and the value of E for  $\text{Ba}^{140}$  was assumed the same as the value of E for  $\text{La}^{140}$ .

The results of the ion exchange experimentation were obtained by collecting 3 liter samples at the inlet to the ion exchange columns, at the cation exchanger effluent, at the anion exchanger effluent, and at the mixed-bed exchanger effluent. These results are tabulated in TABLE IX.

The blank spaces in TABLE IX indicate that either the radioactive isotope had decayed away before counting or that too little was left to form a peak, or that the peak was covered by the spectrum of a higher energy gamma emitter.

The explanation as to why the demineralizer results bounce up and down with the number of passes is somewhat involved. However, the major cause of this effect is due to the poor quality of some of the photopeaks after a substantial amount of the particular radioisotope had been removed. Even though the total number of counts under the photopeak may be large enough so that the statistical variation in this total number is small, the photopeak can still be very ragged and difficult to evaluate quantitatively. However, the important result of the demineralizer study is the value of E for each radioisotope. Since, in general, only a small amount of the radioisotope remained, the value of E was large and, therefore, would not vary very much. The ion exchange efficiency, or fraction of the activity removed by the ion exchangers, is generally much greater

TABLE IX  
RESULTS OF THE ION EXCHANGE EXPERIMENTATION

Nuclide	n	Percentage of Original Concentration Remaining After Passing Through		
		Cation Exchanger	Anion Exchanger	Mixed-Bed Exchanger
Na <sup>24</sup>	43.9	0.0521	0.0606	0.0287
Zn <sup>65</sup>	43.9	90.4	47.3	18.9
Cd <sup>115</sup>	43.9	15.8	3.56	2.53
In <sup>115m</sup>	43.9	15.0	2.78	2.54
La <sup>140</sup>	43.9	84.4	52.7	52.4
Na <sup>24</sup>	236	0.0132	0.0218	0.00910
Zn <sup>65</sup>	236	169		
Cd <sup>115</sup>	236	29.9	3.78	3.94
In <sup>115m</sup>	236	19.5	2.22	2.52
La <sup>140</sup>	236	105	45.1	75.2
Na <sup>24</sup>	641	0.00251	0.00642	0.00604
Zn <sup>65</sup>	641	25.7		
Cd <sup>115</sup>	641	13.7	1.88	1.93
In <sup>115m</sup>	641	30.5	5.64	6.62
La <sup>140</sup>	641	23.3	37.4	52.7
Na <sup>24</sup>	2,240			
Zn <sup>65</sup>	2,240	26.6	9.32	8.30
Cd <sup>115</sup>	2,240	6.39	0.741	0.468
In <sup>115m</sup>	2,240	11.8	4.65	4.34
La <sup>140</sup>	2,240	19.8	8.57	8.57

than the fraction of the activity remaining after passing through the ion exchangers.

The demineralizer studies, despite variations in the results, do show that the cation exchanger removes the greatest quantity of radioactive material in most cases. This may well be due in part to the fact that it is the first column in the series. Cation exchangers are generally placed first since they are more resistant to radiation damage than anion exchangers.<sup>1</sup> However, the anion exchanger obviously is well worth while since it effects a large reduction in the remaining radioactive material, even though the fluid has already passed through the cation exchanger.

The mixed-bed exchanger contributes little or nothing to the removal process. Although this is due in part to the fact that it is the last in the series, the main reason is the difficulty of regeneration. The anion and cation resins in the mixed-bed exchanger have to be separated hydraulically, which is difficult enough, and have to be regenerated separately, which from a practical standpoint, is difficult to carry out with any appreciable success. Thus, it seems that the mixed bed exchanger could be entirely removed with little, if any, decrease in efficiency.

From the results, it is apparent that there is no change in the efficiency of removal of a particular radioactive isotope with time or with its activity, since all the activities reported increased with time. The resistivity of the cooling water is apparently constant in time until the ion exchange medium is saturated.

---

<sup>1</sup>D. W. Moeller, G. W. Leddicotte, and S. A. Reynolds, "Behavior of Radionuclides on Ion Exchange Resins," American Chemical Society Meeting (St. Louis, March 27, 1961).

Studies made by Moeller<sup>1</sup> show graphs of the gross gamma radioactivity as a function of bed depth. In both the cation and anion exchangers the activity is very high near the top of the bed, dropping sharply (by a factor of about 100) to an approximately constant value for the rest of the bed depth. This residual constant activity could be activity that was not removed by the last regeneration. This would explain the apparently constant activity below a certain point.

As further evidence to support the hypothesis of incomplete regeneration, the gross gamma decay curves below the surface of the beds are almost identical. Although the surface decay curve shows an initial decay of shorter half-life activity, the remaining residual activity exhibits the same half-life as the curves taken further down into the bed. Apparently long half-life radioactive isotopes are scattered throughout the beds while the shorter half-life radioactive isotopes are found only near the surface. During regeneration, the bed is thoroughly mixed, thus, accounting for the uniform residual activity throughout the beds due to incomplete regeneration.

Moeller's studies indicate that the ion exchange resins are exhausted from the top down. This means that a different volume of resin would only take a different time to exhaust, and the time of exhaustion would vary directly as the size of the bed. A higher flow rate would reduce the time between regenerations, and a lower flow rate would increase the time between regenerations.

---

<sup>1</sup>D. W. Moeller, Radionuclides in Reactor Cooling Water - Identification, Source and Control, Oak Ridge National Laboratory Report Number 2311, (Oak Ridge, Tennessee: June 12, 1957).

Another possible interpretation of Moeller's data is that the efficiency of ion exchange decreases with an increase in the half-life of the radioactive isotope. TABLE X casts some doubt on this idea. However, the only sure way to prove the hypothesis one way or the other is to take a new resin and put a mixture of radioactive isotopes of the same element through it. If this latter interpretation is correct, then E should be a function of the half-life.

In TABLE X, the effective half-life listed is the half-life of the radioactive isotope itself or the half-life of its parent, if the parent half-life is greater. The value of E was determined by taking an average of the values listed in TABLE IX under the mixed-bed exchanger, dividing by 100, and subtracting from one.

#### Recoil Mechanism Study

As a part of the present study, a neutron activation analysis was made of aluminum with the result that the  $\text{Na}^{23}$  content of aluminum is 20.6 ppm. However, the  $\text{Na}^{23}$  content of aluminum does not significantly contribute to the  $\text{Na}^{24}$  activity of the reactor cooling water since  $\Delta a$  is a constant.  $\Delta a$  will be shown to be a constant later.

As proof of this contention, two aluminum foils identical in size and weight were each thoroughly washed for over an hour in acetone and then for over an hour in demineralized water. These foils were then dried and irradiated in position 2 in hole 71 (about 13" from the bottom of this facility) of the Graphite Reactor for a period of 15 hours. Before irradiation, one foil was covered on both sides by 0.036 inches of cadmium which absorbed all but  $3.37 \times 10^{-5}$  per cent of the thermal neutrons,

TABLE X  
EFFICIENCY OF ION EXCHANGE

Nuclide	Effective Half-Life in Days	E
Na <sup>24</sup>	0.625	1.000
Cd <sup>115</sup>	2.2	0.978
In <sup>115m</sup>	2.2	0.960
La <sup>140</sup>	12.8	0.527
Zn <sup>65</sup>	245	0.864

but only 1.7% of the fission neutron flux. As expected, the two foils had different  $\text{Na}^{24}$  activities;<sup>1</sup> but, after being thoroughly shaken with demineralized water for over an hour after irradiation, the  $\text{Na}^{24}$  activity of the two waters proved to be the same within experimental error (actually the  $\text{Na}^{24}$  activity of the water from the cadmium shielded foil was slightly larger than the activity of the water from the unshielded foil). The aluminum foils were only 0.004" thick, and calculations showed that there was only a negligible reduction in the neutron flux by absorption of neutrons in the sample.

The recoil range of  $\text{Na}^{24}$  produced by the  $(n,\alpha)$  reaction on aluminum will be shown later to be  $5.52 \times 10^{-4}$  centimeters. Thus, the effective thickness<sup>2</sup> of the reaction is  $1.38 \times 10^{-4}$  centimeters.

In order to check this calculation experimentally, the following equation was used:

$$\text{effective thickness} = \left( \frac{A_w}{A_f} \right) \frac{(\text{Thickness of the foil})}{2} \quad (18)$$

where

$A_w$  is the disintegration rate of  $\text{Na}^{24}$  in the water, and

$A_f$  is the disintegration rate of  $\text{Na}^{24}$  in the foil that was cadmium shielded.

The experimental value of the effective thickness turned out to be  $7 \times 10^{-5}$  centimeters  $\pm 25\%$  which does not agree with the calculated value.

Therefore, in order to more nearly approach the conditions actually existing in a nuclear reactor, a foil of the same size and weight

---

<sup>1</sup>The  $\text{Na}^{24}$  activity of the unshielded foil would be a combination of the activity due to the  $(n,\gamma)$  reaction on the sodium in the aluminum plus the activity due to the  $(n,\alpha)$  reaction on aluminum whereas the activity of the shielded foil would be due to the later reaction only.

<sup>2</sup>It will be shown later that the effective thickness is equal to the recoil range divided by four.

as before was placed in 20 cubic centimeters of demineralized water and another polyethylene bottle was filled with 20 cubic centimeters of demineralized water, but no foil. Both bottles were placed in the same position as the foils discussed earlier and irradiated for the same length of time. By subtracting the  $\text{Na}^{24}$  activity in the water that had no foil from the  $\text{Na}^{24}$  activity of the water containing the foil, the activity of the water due to the  $n, \alpha$  reaction on aluminum could be ascertained. This activity turned out to be 17.3 times greater than that observed in the experiments described earlier. This indicates an addition rate that is 17.3 times greater than the addition rate obtained in the previous experimentation. From this latter experiment, the empirical relation

$$r = \phi(\text{area of aluminum})(3.90 \times 10^{-8}) \quad (19)$$

is obtained where  $\phi$  is the neutron flux in neutrons per square centimeter per second. Substituting in the values applicable to the ORR, one obtains a value for  $r$  that is  $4.09 \times 10^{12}$  atoms per second of  $\text{Na}^{24}$  or a value that is 5.74 times too high.<sup>1</sup> Therefore, this type of experimentation is apparently too crude to yield reliable results and, for this reason, should be avoided whenever possible.

---

<sup>1</sup>The presence of aluminum oxide film on the irradiated foil would tend to make the value of  $r$  calculated by equation (19) low rather than high, since the aluminum oxide film is bound to be thicker on the foils than in the ORR since the pH of the foil water was higher. The thickness of the oxide film increases with pH as will be shown later.

## CHAPTER IV

### THEORY

In order to understand what is taking place in a reactor cooling system, it is necessary to become acquainted with the theories involved. Several theories exist, and these will be discussed. In every case, these existing theories have been modified by the author to more exactly coincide with experimental reality. In addition, new theories have been developed by the author to fill in some of the remaining gaps.

Although some of the equations to be discussed will be derived in terms of a water-cooled reactor system, it is obvious that, by appropriate manipulation, they are equally applicable to reactor cooling fluids in general. The reason for talking in terms of a water-cooled system is that this type of system is probably the most readily understood and the simplest to study.

In general, a reactor cooling system may be thought of as a single loop of pipe. The various devices for the removal of radioactive material from the coolant are simply connections to this loop through which a small portion of the coolant is passed. Thus, only a small fraction of the total coolant passes through a clean-up device during any one cycle.

#### Derivation of the Equilibrium Equations for Nuclear Reactor Cooling Fluids

A nuclear reactor cooling system is easier to treat theoretically when the system is at equilibrium. A nuclear reactor cooling system never

comes to equilibrium as far as the specific activities of the respective radioactive isotopes in the cooling system are concerned. However, after a long period of operation, the system will closely approach equilibrium. A theory has been developed by the author that will permit the prediction of equilibrium conditions from data obtained at non equilibrium conditions. The two equations that are developed in this section are valuable as an aid to the better understanding of a reactor cooling system.

#### The Rate of Production Equation

McLain<sup>1</sup> is responsible for the general trend of the following derivation, but it has been modified to some extent in order to be more general in application. If equilibrium conditions are assumed to prevail in a reactor cooling system, then a material balance can be written for the equilibrium specific activity,  $a$ , of a radioactive isotope in the system as follows:<sup>2</sup>

$$\frac{dN}{dT} = 0 = \frac{r}{v} - bEN - \lambda N - cN - GE_G N \quad (20)$$

or

$$a = \frac{r\lambda}{v(bE + \lambda + c + GE_G)} \quad (21)$$

where

$N$  is the number of active nuclei present per milliliter,

$T$  is the time in seconds, and

<sup>1</sup>H. A. McLain, Na<sup>24</sup> Activity in the HFTR Primary Coolant Water, Oak Ridge National Laboratory Central Files Number 60-6-75, (Oak Ridge, Tennessee: June 8, 1960).

<sup>2</sup>The equilibrium specific activity,  $a$ , of a radioactive isotope in a nuclear reactor coolant is by definition directly proportional to the neutron flux which in turn is, by definition, directly proportional to the power of a given nuclear reactor.

$E_G$  is the efficiency of vacuum degasification expressed as a decimal fraction for the particular radioactive isotope in question ( $E_G = 0$  for other than gases).

In a reactor cooling system there may be, in addition to a vacuum degasifier, vents to an off-gas system which is under a slight vacuum. Clearly this will affect only gases in the system. This can best be handled quantitatively by modifying the value of  $E_G$ . In this case,  $E_G$  could have a value greater than 1. A method for determining this modified value of  $E_G$  is given later on.

By definition

$$r = V\Sigma\phi \quad (22)$$

where

$V$  is the volume within which the neutron flux is  $\phi$  in cubic centimeters, and

$\Sigma$  is the macroscopic cross section for the process in units of reciprocal centimeters.

$$\Sigma = \frac{\rho N_0}{A} \sigma \quad (23)$$

where

$\rho$  is the density of the bombarded material in grams per cubic centimeter,  $N_0$  is Avogadro's number ( $6.02 \times 10^{23}$ ) in reciprocal moles,  $\sigma$  is the microscopic cross section for a specific reaction in square centimeters, and

$A$  is the isotopic weight of the bombarded isotope.

### The Specific Activity Equation

Another equation that will be useful for equilibrium conditions in a reactor cooling system is one first developed by Binford.<sup>1</sup> This equation has also been modified in order to be more general in application. When the reactor cooling system is at equilibrium, the increase in specific activity  $\Delta a$  of a radioactive isotope in a reactor cooling system upon passing through the reactor core is equal to the reduction in specific activity by ion exchange, decay, dilution, and degasification.

The specific activity equation is derived in the following manner. The specific activity,  $a_i$ , of the coolant when it is diluted with the make-up water is

$$a_i = (1 - f)a \quad (24)$$

where

$$f \equiv ct. \quad (25)$$

The activity of the coolant when it is diluted with the coolant by-passed through the demineralizers is

$$a_{ii} = (1 - Eg)a_i = (1 - Eg)(1 - f)a \quad (26)$$

where

$$g \equiv bt. \quad (27)$$

The specific activity of the coolant when it is diluted with the coolant by-passed through the vacuum degasifier is

$$a_{iii} = a_{ii}(1 - E_G H) = (1 - Eg)(1 - f)(1 - E_G H)a \quad (28)$$

where

$$H \equiv Gt. \quad (29)$$

---

<sup>1</sup>D. W. Moeller, Radionuclides in Reactor Cooling Water - Identification, Source and Control, Oak Ridge National Laboratory Report Number 2311, (Oak Ridge, Tennessee: June 12, 1957).

Because of decay, the specific activity of the coolant is reduced to

$$a_{iv} = a_{iii} e^{-\lambda t} = (1 - E_g)(1 - f)(1 - E_{GH})ae^{-\lambda t}. \quad (30)$$

Now

$$a = a_{iv} + \Delta a = (1 - E_g)(1 - f)(1 - E_{GH})ae^{-\lambda t} + \Delta a \quad (31)$$

so that

$$\Delta a = a \left[ 1 - (1 - E_g)(1 - f)(1 - E_{GH})e^{-\lambda t} \right] \quad (32)$$

which is the desired specific activity equation.

#### The Non-Equilibrium Equation

Since both equations (21) and (32) are in terms of the specific activity  $a$  of the coolant at equilibrium, it became imperative to develop an equation that would allow calculation of this value of  $a$  from measurements made at non-equilibrium conditions.<sup>1</sup>

First, in order to simplify matters, let us define

$$h \equiv (1 - E_g)(1 - f)(1 - E_{GH})e^{-\lambda t}. \quad (33)$$

Then if  $a_0$  is the initial activity of the coolant, the activity after one cycle will be

$$a_1 = a_0 h + \Delta a. \quad (34)$$

The activity after 2 cycles will be

$$a_2 = a_1 h + \Delta a = (a_0 h + \Delta a)h + \Delta a = a_0 h^2 + \Delta a(1 + h). \quad (35)$$

The activity after 3 cycles will be

$$a_3 = a_2 h + \Delta a = a_0 h^3 + \Delta a(1 + h + h^2). \quad (36)$$

---

<sup>1</sup>Non-equilibrium conditions are with respect to the specific activities in the coolant. Therefore, under non-equilibrium conditions, the specific activities have not yet reached their maximum specific activities.

Therefore, the activity after  $n$  cycles will be

$$\begin{aligned}
 a_n &= a_0 h^n + \Delta a (1 + h + h^2 + \dots + h^{n-1}) \\
 &= a_0 h^n + \Delta a \left( \frac{h^n - 1}{h - 1} \right) \\
 &= a_0 h^n - a (h^n - 1) \\
 &= (a_0 - a) h^n + a. \tag{37}
 \end{aligned}$$

Obviously a plot of  $a_n$  versus  $h^n$  will be a straight line. This contention is experimentally verified in Chapter V. This fact offers a method by which the modified value of  $E_G$  may be ascertained as previously mentioned. If three values of  $a_n$  are obtained, then the value of  $E_G$  may be adjusted by a trial-and-error method until a straight line plot is obtained.

The equilibrium specific activity  $a$  is related to the activity  $a_n$  measured after  $n$  cycles by the relation

$$a = \frac{a_n - a_0 h^n}{1 - h^n}. \tag{38}$$

$a_0$  may be measured at any time after the reactor has reached full power, and  $a_n$  is, of course, measured  $n$  cycles later.

By use of equation (37), it is possible to relate the specific activity of a particular radioactive isotope at any time to its equilibrium specific activity. This is an important development since all experimental values can only be obtained for non-equilibrium conditions. Also, reactors are operated only for finite intervals of time, and the practical quantities of interest may well be quite different from the same quantities evaluated at equilibrium.

Activity Attributable to Recoil Mechanism

Derivation of the Recoil Equation

Schweinler<sup>1</sup> proposed the following derivation of the recoil<sup>2</sup> equation. Consider a rectangular parallelepiped with edges  $dx$ ,  $dy$ ,  $dz$  located inside a material a distance  $x$  from the surface of the material. The area of a sphere is  $4\pi R^2$ , and the area of a zone<sup>3</sup> is  $2\pi R(R - x)$ , so the ratio of the area of the zone to the area of the sphere is  $(R - x)/2R$ . Then of all the recoil nuclei emitted by this rectangular parallelepiped,  $(R - x)/2R$  of them will pass through the surface where  $R$  is the recoil range<sup>4</sup> in centimeters. This is reasonable, since when  $x = 0$ ,  $1/2$  of the particles will pass through the surface, and when  $x = R$ , none of the particles will pass through the surface.

Therefore, in this case,

$$\begin{aligned} r &= \phi \Sigma \int \left( \frac{R - x}{2R} \right) dx dy dz \\ &= \phi \Sigma (\text{area}) \int_0^R \left( \frac{R - x}{2R} \right) dx \\ &= \frac{\phi \Sigma (\text{area}) R}{4} \end{aligned} \quad (39)$$

where the area is in square centimeters.

<sup>1</sup>Interview with H. Schweinler, Theoretical Nuclear Physicist, Solid State Physics Division, Oak Ridge National Laboratory, Oak Ridge, Tennessee, January 4, 1961.

<sup>2</sup>When the bombarding particle has an energy in excess of the threshold energy for a particular nuclear reaction, this excess energy appears as additional kinetic energy of the products of the reaction. The term recoil is used to denote the subsequent movement of the product atom.

<sup>3</sup>Richard Stevens Burington, Handbook of Mathematical Tables and Formulas, (Sandusky, Ohio: Handbook Publishers, Inc., 1956).

<sup>4</sup>The recoil range is simply the straight line distance that the product atom travels after its formation.

## Recoil Range

The next subject of interest is the matter of obtaining a recoil range for the reaction of interest. Nielsen<sup>1</sup> obtained the following theoretical expression for the recoil range:

$$R = \frac{(0.6 \times 10^{-3}) \left( Z_1^{2/3} + Z_2^{2/3} \right)^{1/2} (A_1 + A_2) A_2 E_R}{Z_1 Z_2 A_1 \rho} \quad (40)$$

where

Z is the atomic number,

A is the atomic weight,

$E_R$  is the energy of the recoiling atom in Mev,

the subscript 1 denotes the recoiling atom,

the subscript 2 denotes the matrix material, and

$\rho$  is the density of the matrix material in grams per cubic centimeter.<sup>2</sup>

However, Nielsen claims that equation (40) is not applicable when both  $Z_1 = Z_2$  and  $A_1 = A_2$  since the recoil atoms may lose all of their energy in a head-on collision with a common target atom. Actually the equation agrees with experimental values obtained by Schmitt and Sharp within a factor of two even when this is the case.

## Recoil Energy

Since all the quantities in equation (40) are known with the exception of  $E_R$ , it is necessary to discuss the determination of  $E_R$  for

<sup>1</sup>R. A. Schmitt and R. A. Sharp, "Measurement of the Range of Recoil Atoms," Third Semi-Annual Radiation Effects Symposium, III (October, 1958).

<sup>2</sup>A result of academic interest is the fact that the range in air in centimeters at standard temperature and pressure is equal to the range in aluminum in milligrams per square centimeter times 0.632. For other than conditions of standard temperature and pressure, it is obvious from equation (40) that the range is inversely proportional to the density.

four different kinds of reactions. These four reactions are  $(n,\gamma)$ ,  $(n,f)$ ,  $(n,\alpha)$ , and  $(n,p)$ .

The recoil energy of the nuclide resulting from a slow neutron  $(n,\gamma)$  capture reactions is given by Yosim and Davies<sup>1</sup> to be

$$E_R = \frac{(5.36 \times 10^{-4}) E_\gamma^2}{A_1} \quad (41)$$

where  $E_\gamma$  is the energy of a capture gamma ray in Mev. Unfortunately, neutron capture usually results in the emission of gamma-rays with several different energies, the probability of emission of each energy group differing from that of the others. The probability of emission is the number of capture gammas of that energy emitted per capture. An effective value for  $E_\gamma^2$  can be calculated by multiplying the square of the energy of each capture gamma-ray by its probability of emission and using the sum of these products as the effective value for  $E_\gamma^2$ .

It is known that the total kinetic energy of fission fragments is 162 Mev.<sup>2</sup> If  $E_L$  is the kinetic energy of the light fission fragment in Mev and  $E_H$  is the kinetic energy of the heavy fission fragment in Mev, then

$$E_L + E_H = 162. \quad (42)$$

From the conservation of momentum, we know that

$$A_L E_L = A_H E_H \quad (43)$$

<sup>1</sup>Samuel Yosim and T. H. Davies, "Recoil Atoms from Slow Neutron Capture by Gold and Indium Surfaces," Journal of Physical Chemistry, LVI (1952), pp. 599-603.

<sup>2</sup>Samuel Glasstone and Milton C. Edlund, The Elements of Nuclear Reactor Theory (New York: D. Van Nostrand Company, Inc., 1957).

where

$A_L$  is the mass of the light fission fragment in atomic mass units, and

$A_H$  is the mass of the heavy fission fragment in atomic mass units.

Finally we know that (approximately)

$$A_L + A_H = 234. \quad (44)$$

Therefore, with equations (42), (43), and (44), it is possible to determine the kinetic energy of any fission fragment.

In order to determine the recoil range of fission fragments, it is necessary to refer to Evans.<sup>1</sup> According to Evans, the value of  $Z_1$  should be 20 for Sr<sup>97</sup> and 22 for Xe<sup>138</sup>. In order to be perfectly clear,  $Z_f$  will be used to denote this modification value of  $Z_1$ . In addition, Evans gives experimental data that indicate that, all other things being constant, R should be approximately proportional to  $E_R^x$ , where x has a value slightly greater than 1/2. It was found that this value of x is 0.553. This value was arrived at by using equation (40), substituting  $Z_f$  for  $Z_1$ , and the data of Finkle and others.<sup>2</sup> Finkle gave the range in aluminum in milligrams per square centimeter for Sr<sup>89</sup>, Zr<sup>95</sup>, Ru<sup>103</sup>, Te<sup>129</sup>, I<sup>131</sup>, Ba<sup>140</sup>, Ce<sup>141</sup>, and Ce<sup>144</sup>. In the calculations made here, it was assumed that  $Z_1 = 20 = Z_f$  for all the light fission fragments and that  $Z_1 = 22 = Z_f$  for all the heavy fission fragments. By making this assumption and using the fact that R is directly proportional

<sup>1</sup>Robley D. Evans, The Atomic Nucleus (New York: McGraw-Hill Book Company, Inc., 1955).

<sup>2</sup>B. Finkle and others, "Ranges of Fission-Recoil Fragments of Known Mass Numbers," Radiochemical Studies: The Fission Products, ed. C. D. Coryell and N. Sugarman (New York: McGraw-Hill Book Company, Inc., 1951), IX, Div. IV, 471.

to  $E_R^{0.553}$ , the correct ranges of all these fission fragments in aluminum were predicted with an error of less than 1%. Therefore, in order to calculate the recoil range of fission fragments, the following equation should be used:

$$R = \frac{(0.6 \times 10^{-3}) \left( Z_f^{2/3} + Z_2^{2/3} \right)^{1/2} (A_1 + A_2) A_2 E_R^{0.553}}{Z_f Z_2 A_1 \rho} \quad (45)$$

A method for obtaining a value of  $E_R$  for  $(n,p)$  and  $(n,\alpha)$  reactions is somewhat more complicated. Neutron energy thresholds for endoergic reactions are given by<sup>1</sup>

$$E_T = - \frac{Q(A+1)}{A} \quad (46)$$

where

$E_T$  is the threshold energy in Mev,

$A$  is the atomic weight of the target nuclide, and

the  $Q$  of the reaction in Mev can be calculated from isotopic-mass tables.

If  $Q$  is positive, the reaction is exoergic, and it can occur with slow neutrons; if  $Q$  is negative, the reaction is endoergic and fast neutrons

are required. The reason the threshold energy of the incident neutron

$E_T$ , at which the reaction becomes possible, is actually slightly greater

than  $-Q$ , is because a fraction,  $1/(A+1)$ , of the incident neutron energy

is imparted as translational kinetic energy of the entire compound nucleus.

As the neutron energy  $E_n$  increases, the excess of  $E_n$  over  $E_T$  appears as additional kinetic energy of the products.

---

<sup>1</sup>Robert S. Rochlin, "Fission-Neutron Cross Sections for Threshold Reactions," Nucleonics, XVII (January, 1959), pp. 54-55.

The average neutron energy,  $\bar{E}_n$ , for a particular reaction is given by the following equation:

$$\bar{E}_n = \frac{\int_{E_T}^{\infty} E_n \phi(E_n) \Sigma(E_n) dE_n}{\int_{E_T}^{\infty} \phi(E_n) \Sigma(E_n) dE_n} \quad (47)$$

However,  $\bar{E}_n$  may also be evaluated by the following equation:

$$\bar{E}_n = \frac{\int_{E_T}^{\infty} E_n s(E_n) P(E_n) dE_n}{\int_{E_T}^{\infty} s(E_n) P(E_n) dE_n} \quad (48)$$

where  $s(E_n)$  will be discussed later and

$P(E_n)$  is the penetrability of the barrier that confronts the proton (or alpha-particle) as it emerges from the compound nucleus.<sup>1</sup> The penetrability,  $P(E_n)$ , is given by the following equation:

$$P(E_n) = \left[ \exp\left(\frac{-4zZ_1e^2}{vh}\right) \arccos x^{1/2} - x^{1/2} (1-x)^{1/2} \right] \quad (49)$$

where

$z = 1$  for p,  $2$  for  $\alpha$ ,

$e$  is the electronic charge ( $4.80 \times 10^{-10}$  electrostatic units),

$v$  is the particle velocity in centimeters per second,

$h$  is Planck's constant ( $6.62 \times 10^{-27}$  erg-sec), and

$$x = \frac{E'}{B}. \quad (50)$$

---

<sup>1</sup>D. J. Hughes, Pile Neutron Research (Cambridge 42, Mass.: Addison-Wesley Publishing Company, Inc., 1953).

$E'$  is the particle energy in Mev, and

$B$  is the barrier height in Mev.

Now

$$v = \sqrt{\frac{2E'}{A_P}} \quad (51)$$

where  $E'$  must be converted into ergs by the use of the fact that 1 Mev =  $1.60 \times 10^{-6}$  ergs, and  $A_P$  must be converted into grams by the use of the fact that 1 atomic mass unit =  $1.66 \times 10^{-24}$  grams.

If the kinetic energy acquired by the residual nucleus is neglected, then

$$E' = E_n - E_T. \quad (52)$$

Finally, the empirical relationship for  $B$  given by Hughes is

$$B = 0.96 \frac{z Z_1}{A_2^{1/2}}. \quad (53)$$

The penetrability rises from zero at  $E' = 0$  to unity at  $E' = B$ , and gives the main variation in the cross section in this energy region. Equation (48) can be evaluated graphically. For the  ${}_{13}\text{Al}^{27}(n,\alpha){}_{11}\text{Na}^{24}$  reaction,  $\bar{E}_n = 8.94$  Mev and for the  ${}_{13}\text{Al}^{27}(n,p){}_{12}\text{Mg}^{27}$  reaction,  $\bar{E}_n = 5.16$  Mev.

Since the value of  $\bar{E}_n$  is somewhat in error due to the assumptions made in obtaining the penetrability equation, and since the fission neutron cross sections that will ultimately be used to calculate the value of  $r$  are also uncertain, it would seem to be desirable to find an energy that is reasonably close to  $\bar{E}_n$ , but easier to obtain. Such an energy is the effective threshold energy  $E_e$ .  $E_e$  is slightly less than

$\bar{E}_n$ , but this difference becomes smaller as  $E_e$  and  $\bar{E}_n$  increase. For example, for the  ${}_{13}\text{Al}^{27}(n,\alpha){}_{11}\text{Na}^{24}$  reaction,  $E_e = 8.70$  Mev whereas  $\bar{E}_n = 8.94$  Mev and for the  ${}_{13}\text{Al}^{27}(n,p){}_{12}\text{Mg}^{27}$  reaction,  $E_e = 4.60$  Mev and  $\bar{E}_n = 5.16$  Mev. Since the error introduced by using  $E_e$  in place of  $\bar{E}_n$  is almost certain to be less than the uncertainties in the cross section values, it appears that until better cross section values are available,  $E_e$  can be justifiably used in place of  $\bar{E}_n$ .

Without going into the determination of  $E_e$  for a given reaction, since this is well done by Hughes,<sup>1</sup> it will suffice to say that the meaning of the effective energy is that the correct reaction rate is obtained on the simple assumption that no neutrons with energies below  $E_e$  contribute to the reaction, but all above it do contribute with a constant activation cross section. Thus, the activation cross section is assumed to be zero below  $E_e$  and independent of neutron energy above  $E_e$ . In the determination of the value of  $E_e$ , both the variation of  $\sigma$  with  $E_n$  and the fission neutron spectrum are taken into account.

Using the data of Hughes where the values of  $E_e$  and  $E_T$  are tabulated for a number of (n, $\alpha$ ) and (n,p) reactions, it has been found by the author that

$$E_e - E_T = j Z^i \quad (54)$$

where

$E_e - E_T$  is in Mev,

---

<sup>1</sup>D. J. Hughes, Pile Neutron Research (Cambridge 42, Mass.: Addison-Wesley Publishing Company, Inc., 1953).

$Z$  is the atomic number of the bombarded atom, and the values of the empirical coefficients<sup>1</sup>  $i$  and  $j$  are given in TABLE XI. Equation (54) is accurate within  $\pm 2$  per cent and the maximum observed deviation was less than  $\pm 12$  per cent.

According to Evans,<sup>2</sup> the recoil energy,  $E_R$ , for  $(n,\alpha)$  and  $(n,p)$  reactions, is given by the following equations:

$$\sqrt{E_R} = x \pm \sqrt{x^2 + y} \quad (55)$$

where

$$x \equiv \frac{\sqrt{A_n A_1 E_n}}{A_1 + A_P} \cos \theta \quad (56)$$

$$y \equiv \frac{A_P Q + E_n (A_P - A_n)}{A_1 + A_P} \quad (57)$$

where

$A_n$  is the mass of the incoming neutron (1.01 atomic mass units),

$\theta$  is the angle between the direction the incoming neutron was moving in and the direction the recoiling atom,  $A_1$ , is moving in, and

$A_P$  is the mass of the emitted particle in atomic mass units. In this dissertation, in order to be on the safe side, the maximum recoil energy given by equation (55) will be used. This maximum recoil energy occurs when the positive sign in equation (55) is chosen and when  $\theta$  is assumed to be zero degrees.

---

<sup>1</sup>Since it was found that  $\ln(E_e - E_T)$  versus  $\ln Z$  plots as a straight line for either  $(n,\alpha)$  or  $(n,p)$  reactions within the range of  $Z$  given, the values of  $i$  and  $j$  were determined by least squares analysis.

<sup>2</sup>Robley D. Evans, The Atomic Nucleus (New York: McGraw-Hill Book Company, Inc., 1955).

TABLE XI

COEFFICIENTS FOR THE DETERMINATION OF  $E_e - E_T$ 

	i		j	
	n, $\alpha$	n, p	n, $\alpha$	n, p
$Z \leq 15$	1.16	1.05	0.278	0.170
$Z \geq 15$	0.790	0.755	0.735	0.377

Integration of the Fission NeutronSpectrum Integral

Quite often it is necessary to know the fission neutron flux within a certain energy range. For example, the neutron flux, in a nuclear reactor with neutron energies between 4 and 10 Mev, is often calculated.<sup>1</sup> However, cross sections for threshold reactions are given in terms of the total fission neutron flux over all energies even though the neutrons in the lower energy part of the spectrum may not contribute to the reaction since they have energies below the theoretical threshold energy  $E_T$ .

It should be pointed out here that it is often important to determine how closely the neutron energy spectrum in a certain position in a nuclear reactor corresponds with the fission neutron energy spectrum. Generally above a certain energy (approximately 2 Mev), the correspondence will be very close. In order to determine this energy, it is necessary to use target materials with different threshold energies. The observed fission neutron fluxes should all have the same value. However, as the

---

<sup>1</sup>It would probably be worthwhile to calculate the neutron flux between other energy ranges in addition, such as between 1 and 10 Mev, 2 and 10 Mev, 3 and 10 Mev, etc. As will be explained later, this would allow an estimation of the neutron energy above which the actual neutron energy spectrum coincided with the fission neutron energy spectrum. For the Oak Ridge National Laboratory Research Reactor, this neutron energy is 0.87 Mev.

threshold energy of the target materials becomes lower, the observed fission neutron fluxes begin to diverge from the observed fission neutron fluxes for the target materials with higher threshold energies. Thus, it is possible to determine above what energy the observed and calculated fission neutron energy spectrums coincide.

Because of the steep slope of the fission spectrum above 2 Mev, the effect of moderated neutrons on the spectrum can usually be neglected in the energy range above 2 Mev.<sup>1</sup> Most theoretical threshold energies for fission neutron reactions (reactions caused by fission neutrons) are above 2 Mev.

The energies of the prompt neutrons vary from 15 Mev (the maximum energy observed for fission neutrons) down to thermal values. The energy distribution is called the fission neutron spectrum. The fission neutron spectrum is represented by

$$s(E_n) = k e^{-E_n/l} \sinh \sqrt{mE_n} \quad (58)$$

where

$s(E_n)$  is the number of fission neutrons per unit energy normalized to one fission neutron,

$E_n$  is the neutron energy in Mev, and

$k$ ,  $l$ , and  $m$  have the respective values of  $(2/\pi e)^{1/2}$ , 1, 2 respectively for the Watt Spectrum<sup>2</sup> and 0.454, 0.965, and 2.29 respectively for the

<sup>1</sup>D. J. Hughes, Pile Neutron Research (Cambridge 42, Mass: Addison-Wesley Publishing Company, Inc., 1953).

<sup>2</sup>Samuel Glasstone and Milton C. Edlund, The Elements of Nuclear Reactor Theory (New York: D. Van Nostrand Company, Inc., 1957).

University of California Spectrum.<sup>1</sup>

Equation (58) has been normalized such that

$$\int_0^{\infty} s_W(E_n) dE_n = 1 \quad (59)$$

and

$$\int_0^{14} s_C(E_n) dE_n = 1 \quad (60)$$

where

$s_W(E_n)$  represents the Watt Spectrum, and

$s_C(E_n)$  represents the University of California Spectrum.

Hence, in order to obtain the fission neutron flux within a certain energy range, it is necessary to evaluate the following integral:

$$\int_u^w s(E_n) dE_n = \int_u^w \left( k e^{-E_n/l} \sinh \sqrt{mE_n} \right) dE_n \quad (61)$$

where  $u$  and  $w$  are the lower and upper limits of integration respectively in Mev. Formerly equation (61) was evaluated by numerical integration. However an analytical solution of equation (61) has been developed in this study.

The method of solution is as follows:

$$\begin{aligned} \int_u^w s(E_n) dE_n &= \frac{k}{2} \int_u^w e^{-E_n/l} \left( e^{\sqrt{mE_n}} - e^{-\sqrt{mE_n}} \right) dE_n \\ &= \frac{k}{2} \int_u^w \left[ e^{(\sqrt{mE_n} - E_n/l)} - e^{-(\sqrt{mE_n} + E_n/l)} \right] dE_n \end{aligned}$$

---

<sup>1</sup>Paul Michael Uthe, Jr., Attainment of Neutron Flux Spectra From Foil Activations, Technical Report Number WADC-TR-57-3, (Air Force Institute of Technology, Wright-Patterson Air Force Base, Dayton, Ohio: March, 1957).

$$\begin{aligned}
&= \frac{k}{2} \left[ \int_u^w e^{-(\sqrt{mE_n} - E_n/l)} dE_n - \int_u^w e^{-(\sqrt{mE_n} + E_n/l)} dE_n \right] \\
&= \frac{k}{2} \left\{ \int_u^w e^{\left( \frac{lm}{4} - \left( \sqrt{\frac{E_n}{l}} - \sqrt{\frac{lm}{4}} \right)^2 \right)} dE_n \right. \\
&\quad \left. - \int_u^w e^{-\left( \left( \sqrt{\frac{E_n}{l}} + \sqrt{\frac{lm}{4}} \right)^2 - \frac{lm}{4} \right)} dE_n \right\}. \tag{62}
\end{aligned}$$

Let

$$z = \sqrt{\frac{E_n}{l}} - \sqrt{\frac{lm}{4}} \tag{63}$$

so that

$$E_n = l \left( z + \sqrt{\frac{lm}{4}} \right)^2 \tag{64}$$

and

$$dE_n = 2 \cdot l \left( z + \sqrt{\frac{lm}{4}} \right) dz. \tag{65}$$

The values of  $z$  at the lower and upper limits of integration, respectively, then become

$$U = \sqrt{\frac{u}{l}} - \sqrt{\frac{lm}{4}} \tag{66}$$

and

$$W = \sqrt{\frac{w}{l}} - \sqrt{\frac{lm}{4}}. \tag{67}$$

Let

$$y = \sqrt{\frac{E_n}{l}} + \sqrt{\frac{lm}{4}} \tag{68}$$

so that

$$E_n = l \left( y - \sqrt{\frac{lm}{4}} \right)^2 \tag{69}$$

and

$$dE_n = 2 \cdot 1 \left( y - \sqrt{\frac{lm}{4}} \right) dy. \quad (70)$$

The values of  $y$  at the lower and upper limits of integration, respectively, then become

$$X = \sqrt{\frac{u}{l}} + \sqrt{\frac{lm}{4}} \quad (71)$$

and

$$Y = \sqrt{\frac{w}{l}} + \sqrt{\frac{lm}{4}}. \quad (72)$$

With these substitutions, equation (62) becomes

$$\begin{aligned} \frac{k}{2} & \left[ \int_U^W e^{\frac{lm}{4}} e^{-z^2} 2l \left( z + \sqrt{\frac{lm}{4}} \right) dz - \int_X^Y e^{\frac{lm}{4}} e^{-y^2} 2l \left( y - \sqrt{\frac{lm}{4}} \right) dy \right] \\ & = k l e^{\frac{lm}{4}} \left[ \int_U^W e^{-z^2} \left( z + \sqrt{\frac{lm}{4}} \right) dz - \int_X^Y e^{-y^2} \left( y - \sqrt{\frac{lm}{4}} \right) dy \right] \\ & = k l e^{\frac{lm}{4}} \left\{ \left[ \int_U^W z e^{-z^2} dz + \sqrt{\frac{lm}{4}} \int_U^W e^{-z^2} dz \right] \right. \\ & \quad \left. - \left[ \int_X^Y y e^{-y^2} dy - \sqrt{\frac{lm}{4}} \int_X^Y e^{-y^2} dy \right] \right\}. \quad (73) \end{aligned}$$

According to Sears<sup>1</sup>

$$\begin{aligned} \int_0^x e^{-x^2} dx & = \frac{\sqrt{\pi}}{2} \left\{ 1 - \frac{e^{-x^2}}{\sqrt{\pi x}} \left[ 1 - \frac{1}{2x^2} + \frac{1 \cdot 3}{(2x^2)^2} - \frac{1 \cdot 3 \cdot 5}{(2x^2)^3} + \dots \right] \right\} \\ & = \frac{\sqrt{\pi}}{2} \operatorname{erf}(x) \quad (74) \end{aligned}$$

where  $\operatorname{erf}(x)$  is the error function of  $x$ .

---

<sup>1</sup>Francis Weston Sears, An Introduction to Thermodynamics, The Kinetic Theory of Gases, and Statistical Mechanics (Reading, Massachusetts: Addison-Wesley Publishing Company, Inc. 1956).

Hence equation (73) can be integrated with the result

$$\begin{aligned}
& k_1 e^{\frac{1m}{4}} \left\{ \left[ -\frac{1}{2} \left( e^{-z^2} \begin{vmatrix} W \\ U \end{vmatrix} \right) \right. \right. \\
& \quad \left. \left. + \sqrt{\frac{1m}{4}} \left( \frac{\sqrt{\pi}}{2} \operatorname{erf}(z) \begin{vmatrix} W \\ U \end{vmatrix} \right) \right] \right. \\
& \quad \left. - \left[ -\frac{1}{2} \left( e^{-y^2} \begin{vmatrix} Y \\ X \end{vmatrix} \right) - \sqrt{\frac{1m}{4}} \left( \frac{\sqrt{\pi}}{2} \operatorname{erf}(y) \begin{vmatrix} Y \\ X \end{vmatrix} \right) \right] \right\} \\
& = \frac{k_1}{2} e^{\frac{1m}{4}} \left\{ \left[ \left( e^{-U^2} - e^{-W^2} \right) + \sqrt{\frac{\pi 1m}{4}} \left( \operatorname{erf}(W) - \operatorname{erf}(U) \right) \right] \right. \\
& \quad \left. - \left[ \left( e^{-X^2} - e^{-Y^2} \right) - \sqrt{\frac{\pi 1m}{4}} \left( \operatorname{erf}(Y) - \operatorname{erf}(X) \right) \right] \right\}. \quad (75)
\end{aligned}$$

Therefore, the solution of equation (61) is

$$\begin{aligned}
& \int_u^w \left( k e^{-E_n/1} \sinh \sqrt{mE_n} \right) dE_n \\
& = \frac{k_1}{2} e^{\frac{1m}{4}} \left\{ \left[ \left( e^{-\left(\frac{u}{1} - \sqrt{um} + \frac{1m}{4}\right)} - e^{-\left(\frac{w}{1} - \sqrt{wm} + \frac{1m}{4}\right)} \right) \right. \right. \\
& \quad \left. \left. + \sqrt{\frac{\pi 1m}{4}} \left( \operatorname{erf} \left( \sqrt{\frac{w}{1}} - \sqrt{\frac{1m}{4}} \right) - \operatorname{erf} \left( \sqrt{\frac{u}{1}} - \sqrt{\frac{1m}{4}} \right) \right) \right] \right. \\
& \quad \left. - \left[ \left( e^{-\left(\frac{u}{1} + \sqrt{um} + \frac{1m}{4}\right)} - e^{-\left(\frac{w}{1} + \sqrt{wm} + \frac{1m}{4}\right)} \right) \right. \right. \\
& \quad \left. \left. - \sqrt{\frac{\pi 1m}{4}} \left( \operatorname{erf} \left( \sqrt{\frac{w}{1}} + \sqrt{\frac{1m}{4}} \right) - \operatorname{erf} \left( \sqrt{\frac{u}{1}} + \sqrt{\frac{1m}{4}} \right) \right) \right] \right\}. \quad (76)
\end{aligned}$$

For convenience, several values of  $\operatorname{erf}(x)$  are listed in TABLE XII. An inspection of equation (74) shows that  $\operatorname{erf}(x)$  is undefined for negative values of  $x$ . So the values of  $u$  and  $w$  cannot be less than 0.500 Mev for the Watt Spectrum or less than 0.535 Mev for the University of California Spectrum.

TABLE XII

VALUES OF THE ERROR FUNCTION

x	erf (x)	x	erf (x)
0	0	1.6	0.9763
0.2	0.2227	1.8	0.9891
0.4	0.4284	2.0	0.9953
0.6	0.6039	2.2	0.9981
0.8	0.7421	2.4	0.9993
1.0	0.8427	2.6	0.9998
1.2	0.9103	2.8	0.9999
1.4	0.9523	$\infty$	1.0000

Effective Retention Time

The radioactive isotopes ( $N^{16}$ ,  $N^{17}$ , and  $O^{19}$ ) are produced by activation of the coolant itself. The equations to be developed, in addition to applying to activation of the coolant, will also apply to impurities in the coolant. As will be shown later, the impurities in the coolant of the ORR were so minute that their contribution to the water activity was negligible.

First one starts with the basic equation<sup>1</sup>

$$\Delta A_{\text{T}} = V\Sigma\phi J(1 - e^{-\lambda T}) \quad (77)$$

and introducing equation (23) obtains

$$\Delta A_{\text{T}} = \frac{V\rho N_0\sigma\phi J}{A} (1 - e^{-\lambda T}) = \frac{MN_0\sigma\phi J}{A} (1 - e^{-\lambda T}) \quad (78)$$

where

$\Delta A_{\text{T}}$  is the activity added by nuclear reactions as the coolant passes through the reactor core in disintegrations per second,

M is the mass of the bombarded element in grams,

T is the time of exposure to the neutron flux in seconds, and

J is the percent abundance of an isotope in an element divided by 100.

Now

$$\Delta a = \frac{\Delta A_{\text{T}}}{\text{cubic centimeter of coolant}} \quad (79)$$

and

$$\frac{M}{\text{cubic centimeter of coolant}} = \frac{p}{10^6} \quad (80)$$

---

<sup>1</sup>Samuel Glasstone and Milton C. Edlund, The Elements of Nuclear Reactor Theory (New York: D. Van Nostrand Company, Inc., 1957).

so equation (78) reduces to

$$\Delta a = \frac{p N_0 J \sigma \phi}{10^6 A} (1 - e^{-\lambda T}). \quad (81)$$

If one desires to know the needed retention time for a certain concentration  $p$  of a stable element to produce the observed  $\Delta a$ , one can solve for  $T$  with the result

$$T = -\frac{1}{\lambda} \ln \left( 1 - \frac{\Delta a \cdot 10^6 A}{p N_0 J \sigma \phi} \right). \quad (82)$$

### Burnup Effects

Burnup, as used here, refers to the reduction in the number of target atoms due to their nuclear transmutation by neutron bombardment. A reduction in the number of target atoms would result in a reduction in the production rate of the radioactive isotope under consideration.

If  $N_T$  denotes the number of target atoms, then

$$\frac{dN_T}{dT} = -N_T \sigma \phi \quad (83)$$

and

$$\frac{N_T}{N_{T0}} = e^{-\sigma \phi T} \quad (84)$$

where

$T$  is the exposure time in seconds to the neutron flux, and

$N_{T0}$  is the original number of target atoms at  $T = 0$ .

## CHAPTER V

### CONCLUSIONS

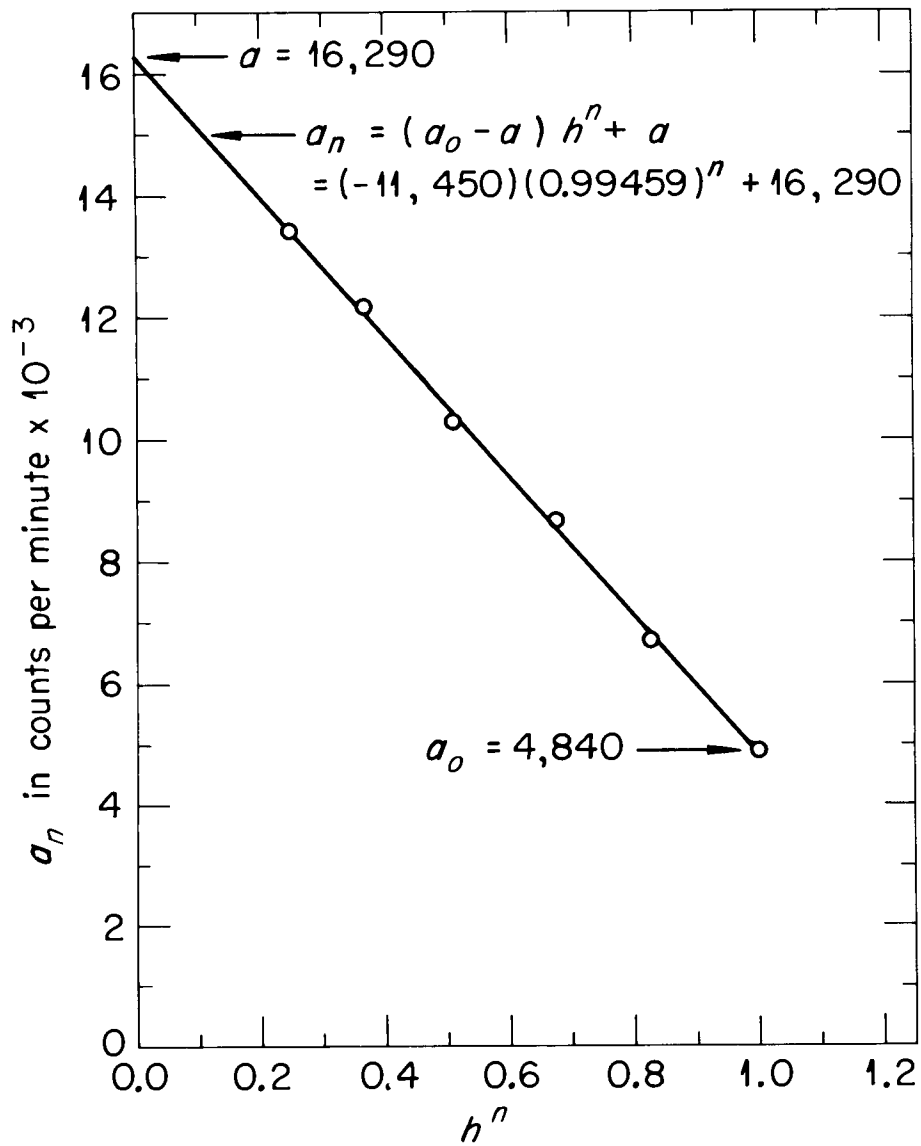
In this Chapter, the discussion will focus on the sources of radioactive isotopes in reactor cooling water and how to predict these activities. With the results of this Chapter and the preceding discussion, it should be possible to predict the activity of almost any radioactive isotope in almost any reactor coolant of almost any type of nuclear reactor.

#### Non-Equilibrium Equation Verification

Equation (37) has been verified experimentally. This has been done by noting that if  $a_n$  (or a quantity proportional to  $a_n$ ) is plotted versus  $h^n$ , the result should be a straight line. When  $h^n = 1$ ,  $a_n = a_0$ , and when  $h^n = 0$ ,  $a_n = a$ . Thus, the slope is  $(a_0 - a)$ . In this experiment, the value of  $b$  was changed to  $1.12 \times 10^{-5}$  reciprocal seconds in order to obtain a more rapid buildup of  $\text{Na}^{24}$ . The experimental results are given in TABLE XIII, and these results are plotted in Graph 1. By least squares analysis, it was determined that the coefficient of correlation was -0.999 (a value of minus one would indicate perfect correlation). The value of  $a_n$  at  $n = \infty$  is the maximum possible value of  $a_n$ . In addition to verification of equation (37) experimentally, several other things can be inferred from the experimental results. In general, the assumption that  $E_G = 0$  for non-gases is verified. The assumption that  $E$  is constant in time and independent of the activity is

TABLE XIII  
BUILDUP OF  $\text{Na}^{24}$  IN THE REACTOR COOLING WATER

n in Cycles	$h^n$	$a_n$ in Counts Per Minute
0.00	1.000	4,900
35.3	0.826	6,700
72.4	0.676	8,680
124	0.510	10,300
184	0.369	12,200
257	0.249	13,400
$\infty$	0.000	16,290 (calculated)

UNCLASSIFIED  
ORNL-LR-DWG. 56479Graph 1. - Buildup of  $\text{Na}^{24}$  in the Reactor  
Cooling Water.

also verified. Finally, the contention that the filters and strainers in the reactor cooling system remove a completely negligible amount of the radioactive material from the coolant is confirmed.

With respect to  $\text{Na}^{24}$ , it is apparent that the assumption that  $\Delta a$  is a constant is well established. Thus,  $r$  is also a constant.

The aluminum surface area exposed to the thermal and fission neutron flux apparently does not vary, as the experimentation with  $\text{Na}^{24}$  showed. ( $\text{Na}^{24}$  is formed by recoil mechanism by the  $n, \alpha$  reaction on aluminum; this will be discussed in more detail later.) The reason for this is that the only difference between the upper and lower parts of the shim rods is that the upper part is filled with cadmium instead of  $\text{U}^{235}$ . Then as the shim rod moves up, the aluminum surface area removed from the thermal and fission neutron fluxes is equal to the aluminum surface area being introduced into the thermal and fission neutron fluxes.

#### Origin of the $\text{Na}^{24}$ Activity

The idea has been advanced that the rate of addition of  $\text{Na}^{24}$  to the cooling water of a reactor with aluminum clad fuel elements is approximately equal to the rate of  $\text{Na}^{24}$  production in the oxide films on these elements. It is assumed that the  $\text{Na}^{24}$  is removed from the oxide film immediately after its formation.

It has been estimated that the thickness of the oxide film on the High Flux Isotope Reactor<sup>1,2</sup> (HFIR) fuel plates will build up after 10 days operation at  $100 \times 10^6$  watts to approximately 1/2 mil for a water

---

<sup>1</sup>The HFIR will have an average fission neutron flux of  $1.43 \times 10^{14}$  neutrons per square centimeter per second.

<sup>2</sup>H. A. McLain,  $\text{Na}^{24}$  Activity in the HFIR Primary Coolant Water, Oak Ridge National Laboratory Central Files Number 60-6-75, (Oak Ridge, Tennessee: June 8, 1960).

pH of 5.0 and 2 mils for a water pH of 7.0. Assuming the density of this film to be 4 grams per cubic centimeter, the composition of this film to be  $\text{Al}_2\text{O}_3 \cdot \text{H}_2\text{O}$ , and the pH of the ORR cooling water to be 6.0, the rate of production of  $\text{Na}^{24}$  in the ORR coolant would be  $9.58 \times 10^{11}$  atoms per second which is reasonably close to the actual value of  $7.14 \times 10^{11}$  atoms per second.

However, the closeness of the results can be very misleading. Since  $r$  has been proven experimentally to be a constant, the oxide film hypothesis does not appear to apply to the ORR. If the oxide film hypothesis did apply, the value of  $r$  would not be a constant since the pH of the cooling water for the ORR varies between approximately 5.5 and 6.5 within a period of one day. Nothing is added to the ORR cooling water for pH control. Therefore, with no evidence to the contrary, it can be assumed that the oxide film hypothesis is invalid with respect to the ORR even though it appears to give the right answer. As will be shown later, the correct reaction rates for the production of  $\text{Na}^{24}$  and  $\text{Mg}^{27}$  are obtained by calculations which neglect any effects attributable to the oxide film. Where the pH of reactor cooling waters is controlled, nitric acid is added in order to prevent oxide film formation on the aluminum. This oxide film reduces the rate of heat transfer and, therefore, is very undesirable. The film builds up faster as the temperature is increased.

#### Origin of the Cadmium Activity

During the course of the hydraulic tests of the ORR core, it was observed that the aluminum-canned cadmium insert in the control rods distorted and restricted water flow through the rods when leaks developed

in the can. This was corrected by providing small holes in the downstream end of the can to relieve any pressure buildup. Thus, even though the cadmium is covered by aluminum, evidently some of the  $\text{Cd}^{115\text{m}}$  and  $\text{Cd}^{115}$  produced eventually passes into the coolant via the small holes in the bottom of the cans. It will be shown later that there is not enough  $\text{Cd}^{114}$  in the coolant to account for the amount of  $\text{Cd}^{115\text{m}}$  and  $\text{Cd}^{115}$  formed. The total area of cadmium in the ORR core is  $1.99 \times 10^4$  square centimeters. A calculation for the recoil ranges of  $\text{Cd}^{115\text{m}}$  and  $\text{Cd}^{115}$  would be subject to great error since the area of the cadmium is covered by aluminum and some of the  $\text{Cd}^{115\text{m}}$  and  $\text{Cd}^{115}$  atoms probably recoil into the aluminum. At any rate, it might be possible to clad the cadmium in such a way that the holes would not be necessary, since the fuel elements do not require holes. This would probably eliminate almost all of the  $\text{Cd}^{115\text{m}}$ ,  $\text{Cd}^{115}$ , and  $\text{In}^{115\text{m}}$  found in the cooling system.

The fission recoil ranges of  $\text{Cd}^{115\text{m}}$  and  $\text{Cd}^{115}$  are essentially the same. The fission yield of  $\text{Cd}^{115\text{m}}$  should be 0.0727 that of  $\text{Cd}^{115}$ , so the value of  $r$  for  $\text{Cd}^{115\text{m}}$  should be 0.0727 times the value of  $r$  for  $\text{Cd}^{115}$ . However, the measured value of  $r$  for  $\text{Cd}^{115\text{m}}$  is actually  $> 2.86$  times that of  $\text{Cd}^{115}$  or  $> 39.3$  times as large as it should be if these two radioactive isotopes were produced mainly by fission. Obviously then, fission is not the major producer of these two radioactive isotopes, but only a negligible producer.

#### Origin of Fission Products

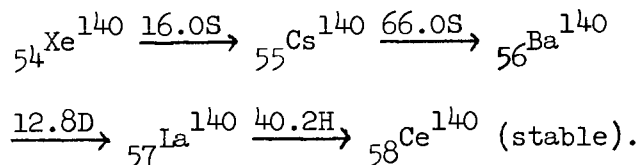
Of the radioactive isotopes listed in TABLE V, only  $\text{Cd}^{115\text{m}}$ ,  $\text{Cd}^{115}$ ,  $\text{In}^{115\text{m}}$ ,  $\text{Ba}^{140}$ , and  $\text{La}^{140}$  might be produced as the result of fission. Of these, only  $\text{Ba}^{140}$  and  $\text{La}^{140}$  have a gaseous parent. Since the fission

yield of  $\text{Cd}^{115\text{m}}$  is only 0.0008% and the fission yield of  $\text{Cd}^{115}$  is only 0.011% (and  $\text{In}^{115\text{m}}$  is the daughter of  $\text{Cd}^{115}$ ), whereas the fission yield of  $\text{Ba}^{140}$  is 6.1% (and  $\text{La}^{140}$  is the daughter of  $\text{Ba}^{140}$ ), by comparing the values of  $r$  given in TABLE VII, it appears that only  $\text{Ba}^{140}$  and  $\text{La}^{140}$  are produced by fission.<sup>1</sup> The method of production of  $\text{Cd}^{115\text{m}}$ ,  $\text{Cd}^{115}$ , and  $\text{In}^{115\text{m}}$  has already been discussed. To further support this contention,  $\text{Ba}^{140}$  can only be formed one other way, that is by a second order ( $n,\gamma$ ) reaction on  $\text{Ba}^{139}$  which would only account for a negligible portion of the  $\text{Ba}^{140}$  produced.

Since the recoil range of  $\text{Ba}^{140}$  in aluminum is only  $1.02 \times 10^{-3}$  centimeters, it obviously does not recoil through the  $3.81 \times 10^{-2}$  centimeter thick fuel cladding.

Assuming that there are  $3.1 \times 10^{10}$  fissions per second per watt of power,<sup>2</sup> then  $5.67 \times 10^{16}$  atoms per second is the total production rate of  $\text{Ba}^{140}$  in the ORR core. Hence, only a small fraction ( $1.03 \times 10^{-7}$ ) of this would have to leak into the cooling water in order to account for the observed  $\text{Ba}^{140}$  activity.

The decay chain leading to  $\text{Ba}^{140}$  is given as a matter of interest:



One hypothesis that might be used to account for the  $\text{Ba}^{140}$  in the water

<sup>1</sup>"Nuclei Formed in Fission: Decay Characteristics, Fission Yields, and Chain Relationships," Journal of the American Chemical Society, LXVIII (1946), pp. 2411-2442.

<sup>2</sup>Samuel Glasstone and Milton C. Edlund, The Elements of Nuclear Reactor Theory (New York: D. Van Nostrand Company, Inc., 1957).

to the apparent exclusion of other fission products (since they were not detected in this study) is that  $\text{Ba}^{140}$  has a gaseous parent. However, this parent ( ${}_{54}\text{Xe}^{140}$ ) has such a short half-life that this can probably be discounted. Also,  $\text{Ba}^{140}$  has a very high fission yield in comparison to most other fission products (only 3 fission products have higher yields, 6.4% being the highest).

Another hypothesis that might be advanced is the possibility of diffusion through the fuel element cladding. However, using the diffusion coefficient for  $\text{Cd}^{112}$  in silver, it was found that the rate of production of  $\text{Ba}^{140}$  by this method would be approximately  $\exp(-10^{25})$  atoms per square cm. per second. Even if the diffusion coefficient of  $\text{Ba}^{140}$  in Al differs by several orders of magnitude from that of  $\text{Cd}^{112}$  in Ag, the diffusion rate would still be insignificant compared to the actual production rate of  $\text{Ba}^{140}$  in the ORR.

It might be supposed that the  $\text{Ba}^{140}$  activity results from the fission of  $\text{U}^{235}$  in the reactor cooling water. However, as will be shown later, this is also a very unlikely source of the  $\text{Ba}^{140}$  activity.

According to Allen,<sup>1</sup> the surface contamination of reactor fuel elements should be less than  $0.013 \times 10^{-6}$  grams of  $\text{U}^{235}$  per square centimeter. This surface contamination occurs as the result of the processes employed in the rolling mills. The same rollers used in rolling the  $\text{U}^{235}$  also roll on the fuel element cladding. Hence, bits of  $\text{U}^{235}$  on the rollers picked up from the  $\text{U}^{235}$  are pressed into the fuel element cladding on the exterior surfaces.

---

<sup>1</sup>V. H. Allen, A Contamination Monitor for Reactor Fuel Rods, Atomic Energy of Canada Limited Report Number 1107, (Chalk River, Ontario, Canada: September, 1960).

As proof of this contention, Emery<sup>1</sup> exposed x-ray film to aluminum processed by the rolling mills and obtained darkening in discrete spots. He cut out some of the contaminated areas, irradiated them with thermal neutrons, and observed a typical fission product gamma-ray spectrum.

It is postulated here that the Ba<sup>140</sup> activity in the cooling water is due to recoil nuclei from these contaminated areas. Therefore, the surface contamination of the fuel element cladding surfaces of the ORR can be calculated.

By means of equation (45) the recoil range of Ba<sup>140</sup> in U<sup>235</sup> is calculated to be  $5.47 \times 10^{-4}$  centimeters. The effective cross section for producing Ba<sup>140</sup> by fission of U<sup>235</sup> is equal to the cross section for fission of U<sup>235</sup> in square centimeters times the fission yield expressed as a decimal fraction. For Ba<sup>140</sup>, this cross section is  $3.6 \times 10^{-23}$  square centimeters. From equation (23), the macroscopic cross section for the process is 1.71 reciprocal centimeters. From equation (39) the area of the U<sup>235</sup> on the exterior of the fuel elements is found to be  $1.88 \times 10^{-1}$  square centimeters. Assuming the thickness is R which is equal to  $5.47 \times 10^{-4}$  centimeters, the volume of U<sup>235</sup> on the exterior of the fuel elements is  $1.03 \times 10^{-4}$  cubic centimeters. Therefore, the surface contamination of the ORR reactor fuel elements appears to be  $4.71 \times 10^{-9}$  grams of U<sup>235</sup> per square centimeter. This is only 36.2% of the maximum permitted value, yet it is enough to account for the total production of Ba<sup>140</sup> in the ORR. Thus, if one determines a value for the surface contamination of the reactor fuel elements, then it should be possible to calculate the equilibrium activity of any fission product in the coolant

---

<sup>1</sup>Interview with J. F. Emery, Chemist, Analytical Chemistry Division, Oak Ridge National Laboratory, Oak Ridge, Tennessee January 4, 1961.

of a reactor using the methods just employed. As a result of this study, this value for the surface contamination appears to be  $4.71 \times 10^{-9}$  grams of  $U^{235}$  per square centimeter of fuel element area.

It is expected that any other radioactive isotopes in the ORR coolant beyond those observed will, in all probability, be fission products. Hence, their activities can be calculated in the same manner.

Possibility of Detecting Fuel Element Rupture  
by Measurement of Delayed Neutrons

From the preceding discussion, it is obvious that very little, if any, of the fission products produced inside a fuel element actually escape into the coolant. It is also apparent that were a fuel element to develop a rupture, the whole reactor cooling system would be badly contaminated with long half-life fission products within a relatively short time. Therefore, it is imperative that the rupture of a fuel element be detected as quickly as possible and before the rupture gets very large. Hence, not only must a proposed detection system be very sensitive, it must also have the capability for rapid response. Since the rupture of a fuel element is most likely at start-up, it must also be able to show a rupture at as low a power level as possible. Above all, it must give a certain indication of a rupture since a false alarm in this respect would prove to be very costly and troublesome.

One method proposed for detection of fuel element ruptures is setting a single-channel analyzer on some selected fission product's gamma-ray peak. Thus, when the peak passed a certain predetermined level, one could infer a fuel element rupture. However, regardless of the gamma-ray energy peak chosen, it is inevitable that many other gamma spectra

would underlie it, all building up at different rates (and all the different rates changing with time). In order to avoid a premature alarm on a system of this sort it is necessary to select the level of activity at which one infers a fuel element rupture at rather a high level. This not only reduces the sensitivity but also involves a longer time lag between rupture and detection. In addition, the apparatus would be almost useless at start up, since the activities are changing at the greatest rates (and unknown rates) at this time.

However, if one uses the principle of delayed-neutron counting, all of the disadvantages of the gamma-ray system are avoided, and all the desired characteristics of a fuel element rupture detection system are obtained.

The delayed neutrons in a reactor are emitted following the beta decay of certain short half-life fission products. The delayed-neutron emitters follow the chemical processes of the element in question. This can result in the delayed neutron being emitted at some point remote from the location of the parent fission event. In the event of a rupture, some delayed neutrons will be emitted by the fission products carried out of the reactor by the coolant flow. These neutrons may be detected as an indication of a fuel element rupture.

There are at least five groups of delayed neutrons which result from  $U^{235}$  fission. These groups are identified in TABLE XIV along with their known or suspected (parenthesized) emitters.<sup>1,2</sup>

---

<sup>1</sup>Samuel Glasstone and Milton C. Edlund, The Elements of Nuclear Reactor Theory (New York: D. Van Nostrand Company, Inc., 1957).

<sup>2</sup>D. C. Pound, Recirculating Gas Loop Rupture Monitoring, HW-51032, (June 20, 1957).

TABLE XIV

PROPERTIES OF DELAYED NEUTRONS IN SLOW-NEUTRON  
FISSION OF URANIUM-235

Group	Half-Life in Seconds	Fraction of Total Fission Neutrons Emitted	Energy of the Emitted Neutron in Mev	Emitter
1	0.430	0.000840	0.420	(Sb <sup>137</sup> , As <sup>85</sup> )
2	1.52	0.00240	0.620	(Sb <sup>135</sup> , I <sup>139</sup> , Tc <sup>136</sup> )
3	4.51	0.00210	0.430	Br <sup>89</sup>
4	22.0	0.00170	0.560	I <sup>137</sup>
5	55.6	0.000260	0.250	Br <sup>87</sup>

In order to calculate the sensitivity of the proposed method for the ORR, the following was assumed:

1. The average thermal neutron flux over the reactor core is  $1.8 \times 10^{14}$  neutrons per square centimeter per second.
2. The flow rate of reactor cooling water through the reactor core is 17,900 gallons per minute.
3. Each  $U^{235}$  nucleus undergoing fission emits a total of 2.5 neutrons on the average.
4. The fission cross section of  $U^{235}$  is 590 barns.<sup>1</sup>
5. The counting rate is double the counting rate due to  $N^{17}$  alone.
6. The  $U^{235}$  has reached a saturation activity as far as delayed neutron emission is concerned.
7. All the other values given in the preceeding discussion are valid.
8. The detection apparatus is the same as that used for the detection of  $N^{17}$ .
9. The efficiency of counting the delayed neutrons is the same as that given for 0.8 Mev neutrons.
10. The counting volume is located 17.3 seconds downstream.
11. The counting rate, due to the 0.9 Mev neutrons of  $N^{17}$ , will be approximately 426 counts per minute  $\pm$  5%.

In order to calculate the sensitivity, it is first necessary to convert the counting rate into specific activity using the counting

---

<sup>1</sup>William H. Sullivan, Trilinear Chart of the Nuclides (New York: John Wiley and Sons, Inc., 1961).

efficiency and counting volume. Then it is necessary to calculate the amount of decay that each neutron group undergoes. This gives a relation between the initial activity and the activity at the counting volume. The next step is to determine the number of neutrons emitted per second per gram of  $U^{235}$  by using equations (22) and (23). In order to obtain the initial specific activity of each delayed neutron group in neutrons per second per gram,  $A_I$ , the following equation is used

$$A_I = r F_f \quad (85)$$

where  $F_f$  is the fraction of total fission neutrons emitted for each delayed neutron group. Each of these values is then divided by the appropriate decay factors to get the specific activity of each group at the counting volume. These values are totaled to obtain the total number of neutrons emitted per second per gram of  $U^{235}$  at the counting volume. This value is divided into the specific activity (in neutrons per second per milliliter), calculated in the first step above, to obtain the sensitivity in terms of grams of  $U^{235}$  per milliliter which can be easily converted into parts per trillion by multiplying by  $10^{12}$ .

Next, the volume rate of flow through the reactor core is converted into milliliters per second by using the appropriate conversion constants. When this value is multiplied by the grams of  $U^{235}$  per milliliter, which was obtained above, the answer in grams of  $U^{235}$  per second is obtained as the sensitivity of the detection apparatus. These calculations show that a leak of  $3.81 \times 10^{-5}$  grams per second of  $U^{235}$  can be detected 17.3 seconds after the initial rupture occurs. This corresponds to a concentration of 33.7 parts per trillion of  $U^{235}$  in the reactor cooling water.

The sensitivity could be increased by the following methods:

1. Location of the counting volume as few seconds downstream from the reactor core as possible.
2. Use of as many  $\text{BF}_3$  tubes as possible.
3. Improvement of the design of the moderating container.
4. Increase of the counting volume.
5. Elimination of glass in the apparatus.<sup>1</sup>

A satisfactory fuel element rupture monitor including four  $\text{BF}_3$  tubes, preamplifier, amplifier discriminator, count rate meter, recorder, alarm, and high voltage supply could be purchased for approximately \$2,000. This is much less than the equivalent gamma-ray equipment would cost.

One further advantage of delayed-neutron counting is that the count rate due to  $\text{N}^{17}$  is directly proportional to the power of the reactor. Then at any power level, the count rate due to  $\text{N}^{17}$  is known and any deviation from this count rate would be an immediate indication of a fuel element rupture.

#### Recoil Mechanism

In this section, it is shown that the methods used in this dissertation to calculate the specific activities of radioactive isotopes produced by  $(n,\alpha)$  and  $(n,p)$  recoil reactions appear to be valid and probably can be used for materials other than aluminum. In order to proceed with this discussion of recoil mechanism, it will be necessary to quote some information from the literature. TABLE XV lists the most up-to-date,

---

<sup>1</sup>Borosilicate glass absorbs neutrons rather strongly.

TABLE XV

THERMAL AND FISSION NEUTRON CROSS SECTIONS FOR  
SEVERAL IMPORTANT REACTIONS

Reaction	Type of Neutron Flux Causing Reaction	Experimentally Measured Microscopic Cross-Section	Theoretically Calculated Microscopic Cross-Section
$^{16}\text{O}(n,p)^{16}\text{N}$	fission	0.0140 mb	0.0150 mb
$^{17}\text{O}(n,p)^{17}\text{N}$	fission	0.00930 mb	
$^{18}\text{O}(n,\gamma)^{19}\text{O}$	thermal	$0.210 \pm 0.040$ mb	
$^{27}\text{Al}(n,\alpha)^{24}\text{Na}$	fission	0.600 mb	1.45 mb
$^{27}\text{Al}(n,p)^{27}\text{Mg}$	fission	3.42 mb	3.91 mb
$^{27}\text{Al}(n,\gamma)^{28}\text{Al}$	thermal	$0.210 \pm 0.040$ b	
$^{27}\text{Al}(n,\gamma)^{28}\text{Al}$	fission	0.370 mb	0.270 mb
$^{64}\text{Zn}(n,\gamma)^{65}\text{Zn}$	thermal	$0.500 \pm 0.100$ b	
$^{114}\text{Cd}(n,\gamma)^{115\text{m}}\text{Cd}$	thermal	$0.140 \pm 0.030$ b	
$^{114}\text{Cd}(n,\gamma)^{115}\text{Cd}$	thermal	$1.10 \pm 0.30$ b	
$^{115}\text{Cd} \rightarrow ^{115\text{m}}\text{In} + \beta^-$			
$^{235}\text{U}(n,f)^{140}\text{Ba}$	thermal	36.0 b	
$^{140}\text{Ba} \rightarrow ^{140}\text{La} + \beta^-$			

self-consistent set of data taken from several sources.<sup>1,2,3,4,5,6,7,8,9</sup> The microscopic cross sections are listed in terms of barns (b) or millibarns (mb) where one barn =  $10^{-24}$  square centimeters. The theoretically calculated microscopic cross sections are listed for interest only and were not used in the calculations.

TABLE XVI lists the percent abundance and the atomic weight of several isotopes of interest.<sup>10</sup> TABLE XVII lists values of  $Q$ ,  $E_T$ , and  $E_e$

<sup>1</sup>N. Faull, An Experimental Study of Neutron Induced Activities in Water, Atomic Energy Research Establishment Report Number 1919, (Harwell, Berks., England: 1957).

<sup>2</sup>Robert S. Rochlin, "Fission-Neutron Cross Sections for Threshold Reactions," Nucleonics, XVII (January, 1959), pp. 54-55.

<sup>3</sup>D. J. Hughes, Pile Neutron Research (Cambridge 42, Mass.: Addison-Wesley Publishing Company, Inc., 1953).

<sup>4</sup>Charles D. Hodgman, Robert C. Weast, and Samuel M. Selby, Handbook of Chemistry and Physics (Cleveland, Ohio: Chemical Rubber Publishing Co., 1958).

<sup>5</sup>Paul A. Roys and Kalman Shure, "Production Cross Section of  $N^{16}$  and  $N^{17}$ ," Nuclear Science and Engineering, IV (1958), pp. 536-545.

<sup>6</sup>R. Hinves and K. Parker, Average Cross-Sections for Fission Spectrum Neutrons, United Kingdom Atomic Energy Authority, Atomic Weapons Research Establishment Report Number O-2/60, (Aldermaston, Berkshire, England: April, 1960).

<sup>7</sup>C. E. Mellish, "Threshold" Reaction Cross-Sections in Reactors - An Intercomparison, United Kingdom Atomic Energy Authority, Atomic Energy Research Establishment Report Number R 3251, (Harwell, Berkshire, England: February, 1960).

<sup>8</sup>J. W. Baum, Neutron Dosimetry - A Review, The University of Rochester Report Number 381, (Rochester, New York: March 29, 1955).

<sup>9</sup>T. O. Passell and R. L. Heath, Fission Neutron Cross Section Measurements for Threshold Reactions: Nickel as a Useful Fast Flux Monitor, Phillips Petroleum Co., (Idaho Falls, Idaho: October 14, 1959).

<sup>10</sup>James M. Cork, Radioactivity and Nuclear Physics (New York: D. Van Nostrand Company, Inc., 1957).

TABLE XVI

PERCENT ABUNDANCE AND ATOMIC WEIGHT OF SEVERAL ISOTOPES

Isotope	Percent Abundance	Atomic Weight in Atomic Mass Units
${}^1_1\text{H}^1$		1.01
${}^4_2\text{He}^4$		4.00
${}^{16}_8\text{O}$	99.8	16.0
${}^{17}_8\text{O}$	0.0390	17.0
${}^{18}_8\text{O}$	0.204	18.0
${}^{23}_{11}\text{Na}$	100	23.0
${}^{24}_{11}\text{Na}$		24.0
${}^{26}_{12}\text{Mg}$	11.3	26.0
${}^{27}_{12}\text{Mg}$		27.0
${}^{27}_{13}\text{Al}$	100	27.0
${}^{28}_{13}\text{Al}$		28.0
${}^{64}_{30}\text{Zn}$	48.9	63.9
${}^{65}_{30}\text{Zn}$		64.9
${}^{114}_{48}\text{Cd}$	28.9	114
${}^{115\text{m}}_{48}\text{Cd}$		115
${}^{115}_{48}\text{Cd}$		115
${}^{140}_{56}\text{Ba}$		140
${}^{235}_{92}\text{U}$		235

TABLE XVII

VALUES OF Q,  $E_T$ , AND  $E_e$  FOR SEVERAL FISSION  
NEUTRON REACTIONS

Reaction	Q in Mev	$E_T$ in Mev	$E_e$ in Mev
$O^{16}(n,p)N^{16}$	- 9.50	10.22	11.7
$O^{17}(n,p)N^{17}$	- 8.00	8.47	10.0
$Al^{27}(n,\alpha)Na^{24}$	- 3.18	3.27	8.70
$Al^{27}(n,p)Mg^{27}$	- 2.03	2.10	4.60
$Al^{27}(n,\gamma)Al^{28}$	+ 7.70		

for several fission neutron reactions which were obtained from some of the same sources cited for microscopic cross sections. TABLE XVIII lists the recoil ranges of several important reactions. The recoil ranges of  $\text{Na}^{24}$  and  $\text{Mg}^{27}$  were calculated by means of equations (40) and (55). The recoil range of  $\text{Ba}^{140}$  was calculated using equation (45). Equations (40) and (41) were used along with the experimental data of Troubetzkoy and Goldstein<sup>1</sup> to calculate the range of  $\text{Al}^{28}$  for the thermal neutron reaction. The information in TABLE XVI was used in the calculation of the recoil ranges of  $\text{Na}^{24}$ ,  $\text{Mg}^{27}$ ,  $\text{Al}^{28}$  (thermal), and  $\text{Ba}^{140}$ .

The  $\text{Al}^{28}$  produced in the cooling fluid by the thermal neutron reaction accounts for only 4.3% of the  $\text{Al}^{28}$  produced. The remaining 95.7% of the  $\text{Al}^{28}$  produced is produced by the fission neutron recoil reaction. If this is assumed to be the case, then from the experimental data, the recoil range for the fission neutron  $(n,\gamma)$  reaction on  $\text{Al}^{27}$  is the range listed in TABLE XVIII. This range corresponds to a recoil energy of 4.19 Mev.

The capture gamma-rays of the fission neutron reaction  $\text{Al}^{27}(n,\gamma)\text{Al}^{28}$  are expected to be quite different from those for the same reaction induced by thermal neutrons. Since experiments at other than thermal energies are quite difficult, especially with the light nuclei for which the changes are expected to be the most significant, it is not likely that any large volume of information of such fluctuations will become available in the future.

---

<sup>1</sup>E. Troubetzkoy and H. Goldstein, A Compilation of Information on Gamma-Ray Spectra Resulting From Thermal-Neutron Capture, Oak Ridge National Laboratory Report Number 2904, (Oak Ridge, Tennessee: May 17, 1960).

TABLE XVIII  
RECOIL RANGES

Reaction	Type of Neutron Flux Causing Reaction	Recoil Range in Centimeters in Reactant
$\text{Al}^{27}(\text{n},\alpha)\text{Na}^{24}$	fission	$5.75 \times 10^{-4}$
$\text{Al}^{27}(\text{n},\text{p})\text{Mg}^{27}$	fission	$1.43 \times 10^{-4}$
$\text{Al}^{27}(\text{n},\gamma)\text{Al}^{28}$	thermal	$1.10 \times 10^{-7}$
$\text{Al}^{27}(\text{n},\gamma)\text{Al}^{28}$	fission	$9.70 \times 10^{-4}$
$\text{U}^{235}(\text{n},\text{f})\text{Ba}^{140}$	thermal	$5.47 \times 10^{-4}$

TABLE XIX lists the observed and calculated values of  $r$  for  $\text{Na}^{24}$  and  $\text{Mg}^{27}$ . In every case, the errors in the calculated values of  $r$  can be attributed to errors in the microscopic cross sections used in the calculations.

Compensation of Burnup of  $\text{U}^{235}$  Contamination  
by Shim Rod Movement

The most likely place where burnup might have an effect on the production rate is the burnup of the  $\text{U}^{235}$  contamination on the reactor fuel element cladding. Since a fuel element is normally left in the reactor for a maximum of 55.8 days, then  $N_T/N_{T0}$  for this process is 0.600.

Before going any further with this discussion, it should be noted that the aluminum clad shim rods have a cadmium neutron absorber section at the top and a  $\text{U}^{235}$  fuel section at the bottom. In order to keep the reactor power level constant, the shim rods are continuously moving upwards to compensate for burnup of the  $\text{U}^{235}$  in the fuel elements. Thus, even though the  $\text{U}^{235}$  on the exterior of the stationary fuel elements is being reduced, new surface area is being introduced into the reactor at a rate which tends to compensate for the burnup of  $\text{U}^{235}$  on the external surfaces of the fuel elements. By following the buildup of  $\text{La}^{140}$  in the reactor over a period where the calculated burnup would have been 5%, it was found that the observed points fell on the straight line calculated on the assumption of a constant production rate. It appears, therefore, that within the accuracy of the measurements, the production rate of  $\text{La}^{140}$  was constant.

TABLE XIX

OBSERVED AND CALCULATED RATES OF PRODUCTION  
OF Na<sup>24</sup> AND Mg<sup>27</sup> IN THE COOLING WATER

Nuclide	r in Atoms per Second (observed)	r in Atoms per Second (calculated using $E_e$ )	r in Atoms per Second (calculated using $\bar{E}_n$ )
Na <sup>24</sup>	$7.14 \times 10^{11}$	$5.24 \times 10^{11}$	$5.45 \times 10^{11}$
Mg <sup>27</sup>	$7.31 \times 10^{11}$	$6.59 \times 10^{11}$	$7.76 \times 10^{11}$

TABLE XX lists the data which verify the preceding statement. Each sample was counted for 10 minutes. The value of  $g$  in equation (33) was 0.00250 for this set of measurements. The calculated values of  $a_n$  in TABLE XX were calculated from the observed values of  $a_n$  at  $n = 43.9$  and  $n = 236$  using equation (37). Obviously, the agreement between the calculated and the observed values of  $a_n$  is excellent.

The data in TABLE XX also verify the fact that equation (37) is valid for daughter radioactive isotopes as long as the half-life of the parent is used in the calculations if the parent half-life is greater than the daughter half-life. It also implies that the so-called plating out of radioactive isotopes on the walls of the cooling system is insignificant compared to other methods of removal, at least for  $Ba^{140}$  and  $La^{140}$ , and most likely for all the other radioactive isotopes as well. The data in TABLE XIII implies that plating out of  $Na^{24}$  is insignificant compared to other methods of removal. Actually none of the radioactive isotopes listed in TABLE VII showed any significant plating out tendencies. Even if radioactive isotopes were observed on the walls of the cooling system, it appears that, in general, plating out is negligible in comparison with the other means by which radioactive isotopes are removed from the cooling system of a nuclear reactor.

Calculations have shown that burnup of the material being activated has a completely negligible effect on the rate of production of radioactive isotopes in the cooling water with respect to activation of the coolant itself and the fuel element cladding (where radioactive isotopes are added to the water by recoil mechanism).

TABLE XX  
BUILDUP OF  $\text{La}^{140}$  IN THE REACTOR COOLING WATER

n in Cycles	$h^n$	$a_n$ in Counts Per Minute (Observed)	$a_n$ in Counts Per Minute (Calculated)
0.00	1.000		260
43.9	0.934	334	
236	0.685	608	
641	0.358	968	966
2240	0.0278	1,330	1,330
$\infty$	0.000		1,360

Effective Fission Flux Retention Time

Offhand, one might expect that the effective fission flux retention time would be very nearly the same as the actual retention time, since the fission neutron flux is rapidly moderated down to lower energies and would not extend far beyond the actual reactor core. Since  $N^{16}$  and  $N^{17}$  are produced by the fission neutron flux, calculations were made to determine what the activity should be if the effective retention time were equal to the actual retention time. On this basis, the value of  $\Delta a$  for  $N^{16}$  was calculated to be  $6.81 \times 10^5$  disintegrations per second per milliliter which is only 4.55% above the observed value of  $\Delta a$  of  $6.50 \times 10^5$  disintegrations per second per milliliter. Also, on the same basis, the value of  $\Delta a$  for  $N^{17}$  was calculated to be  $2.93 \times 10^2$  disintegrations per second per milliliter which is 59% below the observed activity of  $5.38 \times 10^2$  disintegrations per second per milliliter. Since the differences between these values of  $\Delta a$  are no greater than those to be expected in view of the uncertainties in the microscopic cross sections used in the calculations, it seems that the actual retention time can be used in calculations involving fission neutron flux reactions.

Effective Thermal Flux Retention Time

It might be expected that the effective thermal flux retention time might be somewhat greater than the actual or effective fission neutron flux retention time since the reduction in thermal flux outside of the core is partly compensated for by moderation of the fission neutron

flux down to thermal energies.<sup>1</sup> Hence, the thermal flux might be effective over a volume slightly larger than the actual coolant volume of the core. Of course the effect would depend on the size of the reactor core.

If one uses the value of  $\Delta a$  for  $O^{19}$  to calculate the effective thermal flux retention time, the result is a value of 1.29 seconds or 21.4 times as long as the actual or effective fission neutron flux retention time. However, it is extremely doubtful that this is the case. Apparently some unknown factor is responsible for the fact that the value of  $\Delta a$  for  $O^{19}$  is 21.4 times larger than the calculated value of  $\Delta a$  for  $O^{19}$ . As a general rule, it might be wise to multiply the calculated value of  $\Delta a$  for  $O^{19}$  by 21.4 to be on the safe side when computing the activity of  $O^{19}$  in other reactors.

TABLE XX lists the effective thermal flux retention times needed in order for the stable element concentration to account for the observed value of  $\Delta a$  of its radioactive isotope. Clearly, all of the impurities are present in amounts that are negligible as far as the value of  $\Delta a$  of the coolant is concerned.

A calculation was made using the value of 1.29 seconds to determine what concentration of zinc would be needed to account for the observed  $\Delta a$ . The concentration required was 0.713 parts per million,

---

<sup>1</sup>This effect has been experimentally observed. In an unpublished study made by the author on the University of Oklahoma nuclear reactor, the experimentally measured thermal neutron flux in the cooling water did not decrease with increasing distance from the core as rapidly as a pure thermal neutron flux would have. The thermal neutron flux measurements were determined from the activities of indium foils placed in the cooling water at various distances from the reactor core which very closely approximated a plane neutron source. Hence, part of the experimentally determined thermal neutron flux was due to moderation of the fission neutron flux to thermal energies. A later investigation employing a different approach yielded the same results.

TABLE XXI

REQUIRED EFFECTIVE THERMAL NEUTRON FLUX RETENTION  
TIMES FOR SEVERAL RADIOACTIVE ISOTOPES

Radioactive Isotope	Effective Retention Time in seconds required to attain the observed activity
Na <sup>24</sup>	43.5
Mg <sup>27</sup>	$\geq 45.1$
Al <sup>28</sup>	48.0
Cd <sup>115m</sup>	2340
Cd <sup>115</sup>	105
Ba <sup>140</sup>	$\gg 1.24 \times 10^{-1}$

and since it has been shown that the actual concentration of zinc is  $\ll 0.1$  parts per million, it is evident that the  $\text{Zn}^{65}$  observed is not due to the activation of stable zinc in the coolant.

The method of production of  $\text{Zn}^{65}$  in the reactor cooling water is still unknown. It has been shown that there is not enough stable  $\text{Zn}^{64}$  in the reactor cooling water to account for its activity. Also, there is supposed to be no  $\text{Zn}^{64}$  in the reactor core. It is possible that some experimental apparatus in the ORR contains enough zinc to account for the observed activity. Fortunately, its equilibrium activity is rather low (only  $\text{Ba}^{140}$  and  $\text{La}^{140}$  are lower).

The value for  $\text{Ba}^{140}$  was calculated on the basis of  $\text{U}^{235}$  in the coolant, but if the  $\text{U}^{235}$  had been present, the delayed neutrons would have shown up in the determination of the half-life of  $\text{N}^{17}$ .

#### Summary

The calculated value of the  $\text{U}^{235}$  contamination on the reactor fuel elements was 36.2% of the maximum permitted value. These calculations indicate that it is probably relatively easy to keep the actual contamination below this maximum value. With the experimental apparatus used, it was not possible to detect any fission products other than  $\text{Ba}^{140}$  and  $\text{La}^{140}$ . If other fission products had been observed, it would have been possible to check the equations used in the calculations of the rate of production of fission products directly.

The rate of production of radioactive isotopes produced by recoil mechanism was calculated by using equation (39) with the appropriate calculated values for  $n, \alpha$  and  $n, p$  reactions. The calculated

value of  $r$  for the  $\text{Al}^{27}(n,\alpha)\text{Mg}^{27}$  reaction was 5.97% above the observed value. The errors involved can be attributed to uncertainties in the microscopic cross sections.

It is expected that the methods of prediction used will be superior to simulated experimental methods, since it was demonstrated that it is difficult to experimentally simulate actual conditions in a nuclear reactor.

The value of  $\Delta a$  for activation of the coolant or impurities in the coolant can be calculated by means of equation (81). For  $\text{N}^{16}$ , the calculated value of  $\Delta a$  was 4.55% above the observed value, whereas for  $\text{N}^{17}$  the calculated value was 59% below the observed value. Here again the errors in both cases can be attributed to errors in the microscopic cross sections used in the calculations.

The theory used in predicting the radioactivity of nuclear reactor cooling fluids is a general theory. It would be desirable to apply this theory to other nuclear reactors, since the principles used in deriving the theory are basic to almost all reactors. The equations have been verified successfully, with the expected experimental error for one reactor, the ORR.

## BIBLIOGRAPHY

### Books

- Hughes, D. J. Pile Neutron Research. Cambridge 42, Mass.: Addison-Wesley Publishing Company, Inc., 1953.
- Burington, Richard S. Handbook of Mathematical Tables and Formulas. Sandusky, Ohio: Handbook Publishers, Inc., 1956.
- Glasstone, Samuel and Edlund, Milton C. The Elements of Nuclear Reactor Theory. New York: D. Van Nostrand Company, Inc., 1957.
- Sears, Francis W. An Introduction to Thermodynamics, The Kinetic Theory of Gases, and Statistical Mechanics. Reading, Massachusetts: Addison-Wesley Publishing Company, Inc., 1956
- Directory of Nuclear Reactors. Vol. I: Power Reactors. Karntner Ring, Vienna 1, Austria: The International Atomic Energy Agency, 1959.
- Directory of Nuclear Reactors. Vol. II: Research, Test, and Experimental Reactors. Karntner Ring, Vienna 1, Austria: The International Atomic Energy Agency, 1959.
- Washburn, Edward W. and others. International Critical Tables. Vol. III. New York: McGraw-Hill Book Company, 1928, p. 255.
- Daniels, Farrington and Alberty, Robert A. Physical Chemistry. New York: John Wiley and Sons, Inc., 1958.
- Evans, Robley D. The Atomic Nucleus. New York: McGraw-Hill Book Company, Inc., 1955.
- Bleuler, Ernst and Goldsmith, George J. Experimental Nucleonics. New York: Rinehart and Company, Inc., 1956.
- Cork, James M. Radioactivity and Nuclear Physics. New York: D. Van Nostrand Company, Inc., 1957.
- Crouthamel, C. E. Applied Gamma-Ray Spectrometry. New York: Pergamon Press, 1960.
- Kinsman, Simon and others. Radiological Health Handbook. Cincinnati, Ohio: Robert A. Taft Sanitary Engineering Center, 1957.
- Hodgman, Charles D., Weast, Robert C. and Selby, Samuel M. Handbook of Chemistry and Physics. Cleveland, Ohio: Chemical Rubber Publishing Co., 1958.

Fair, Gordon M. and Geyer, John C. Water Supply and Waste-Water Disposal. New York: John Wiley and Sons, Inc., 1956.

Sullivan, William H. Trilinear Chart of the Nuclides. New York: John Wiley and Sons, Inc., 1961.

#### Reports

McLain, H. A.  $\text{Na}^{24}$  Activity in the HFIR Primary Coolant Water, Oak Ridge National Laboratories Central Files Number 60-6-75, Oak Ridge, Tennessee, June 8, 1960.

Moeller, D. W. Radionuclides in Reactor Cooling Water - Identification, Source and Control, Oak Ridge National Laboratory Report Number 2311, Oak Ridge, Tennessee, June 12, 1957.

Faull, N. An Experimental Study of Neutron Induced Activities in Water, Atomic Energy Research Establishment Report Number 1919, Harwell, Berks., England, 1957.

Uthe, Paul Michael, Jr. Attainment of Neutron Flux Spectra From Foil Activations, Technical Report Number WADC-TR-57-3, Air Force Institute of Technology, Wright-Patterson Air Force Base, Dayton, Ohio, March, 1957.

Cole, T. E. and Gill, J. P. The Oak Ridge National Laboratory Research Reactor (ORR) - A General Description, Oak Ridge National Laboratory Report Number 2240, Oak Ridge, Tennessee, January 21, 1957.

Heath, R. L. Scintillation Spectrometry Gamma-Ray Spectrum Catalogue, Phillips Petroleum Co. Report Number IDO-16408, Idaho Falls, Idaho, July 1, 1957.

Pound, D. C. Recirculating Gas Loop Rupture Monitoring, HW-51032, June 20, 1957.

Allen, V. H. A Contamination Monitor for Reactor Fuel Rods, Atomic Energy of Canada Limited Report Number 1107, Chalk River, Ontario, Canada, September, 1960.

Hinves, R. and Parker K. Average Cross-Sections for Fission Spectrum Neutrons, United Kingdom Atomic Energy Authority, Atomic Weapons Research Establishment Report Number O-2/60, Aldermaston, Berkshire, England, April, 1960.

Mellish, C. E. "Threshold" Reaction Cross-Sections in Reactors - An Intercomparison, United Kingdom Atomic Energy Authority, Atomic Energy Research Establishment Report Number R 3251, Harwell, Berkshire, England, February, 1960.

- Baum, J. W. Neutron Dosimetry - A Review, The University of Rochester Report Number 381, Rochester, New York, March 29, 1955.
- Passell, T. O. and Heath, R. L. Fission Neutron Cross Section Measurements for Threshold Reactions: Nickel as a Useful Fast Flux Monitor, Phillips Petroleum Co., Idaho Falls, Idaho, October 14, 1959.
- Troubetzkoy, E. and Goldstein, H. A Compilation of Information on Gamma-Ray Spectra Resulting From Thermal-Neutron Capture, Oak Ridge National Laboratory Report Number 2904, Oak Ridge, Tennessee

#### Articles

- Schmitt, R. A. and Sharp, R. A. "Measurement of the Range of Recoil Atoms," Third Semi-Annual Radiation Effects Symposium, III, October, 1958.
- Yosim, Samuel and Davies, T. H. "Recoil Atoms from Slow Neutron Capture by Gold and Indium Surfaces," Journal of Physical Chemistry, LVI, 1952, pp. 599-603.
- Finkle, B. and others. "Ranges of Fission-Recoil Fragments of Known Mass Numbers," Radiochemical Studies: The Fission Products, ed. C. D. Coryell and N. Sugarman, New York: McGraw-Hill Book Company, Inc., IX, Div. IV, 1951, p. 471.
- Rochlin, Robert S. "Fission-Neutron Cross Sections for Threshold Reactions," Nucleonics, XVII. January, 1959, pp. 54-55.
- Strominger, D., Hollander, J. M., and Seaborg, G. T. "Table of Isotopes," Reviews of Modern Physics, XXX, Part II, April, 1958, pp. 585-904.
- Moeller, D. W., Leddicotte, G. W. and Reynolds, S. A. "Behavior of Radio-nuclides on Ion Exchange Resins," American Chemical Society Meeting, Saint Louis, March 27, 1961.
- "Nuclei Formed in Fission: Decay Characteristics, Fission Yields, and Chain Relationships," Journal of the American Chemical Society, LXVIII, 1946, pp. 2411-2442.
- Roys, Paul A. and Shure, K. "Production Cross Section of  $N^{16}$  and  $N^{17}$ ," Nuclear Science and Engineering, IV, 1958, pp. 536-545.

#### Interviews

- Interview with H. Schweinler, Theoretical Nuclear Physicist, Solid State Physics Division, Oak Ridge National Laboratory, Oak Ridge, Tennessee, January 4, 1961.

Interview with J. F. Emery, Chemist, Analytical Chemistry Division, Oak Ridge National Laboratory, Oak Ridge, Tennessee, January 4, 1961.

## APPENDIX

### Glossary of Principal Symbols

#### English Letters

A	Isotopic weight of a bombarded isotope
$A_f$	Disintegration rate of $\text{Na}^{24}$ in a foil that was cadmium shielded
$A_H$	Mass of a heavy fission fragment in atomic mass units
$A_L$	Mass of a light fission fragment in atomic mass units
$A_n$	Mass of an incoming neutron
$A_p$	Mass of an emitted particle in atomic mass units
$A_w$	Disintegration rate of $\text{Na}^{24}$ in water
$\Delta A_T$	Activity added by nuclear reactions as a coolant passes through a reactor core in disintegrations per second
a	Equilibrium specific activity of a radioactive isotope in disintegrations per second per milliliter of reactor coolant
$a_0$	Initial specific activity of a coolant in disintegrations per second per milliliter at $n = 0$
$a_n$	Specific activity of a radioactive isotope in disintegrations per second per milliliter of reactor coolant at $n$ cycles
$\Delta a$	Change in the specific activity of a coolant at equilibrium on passing through a reactor core in disintegrations per second per milliliter of reactor cooling fluid
B	A constant for any specific solvent and solute
b	Flow rate through the demineralizers in milliliters per second divided by $v$
C	Area under a photo-peak in counts per second
c	Make-up flow rate in milliliters per second divided by $v$
D	Partial latent heat of vaporization of a gas from a solution in joules per gram-mole

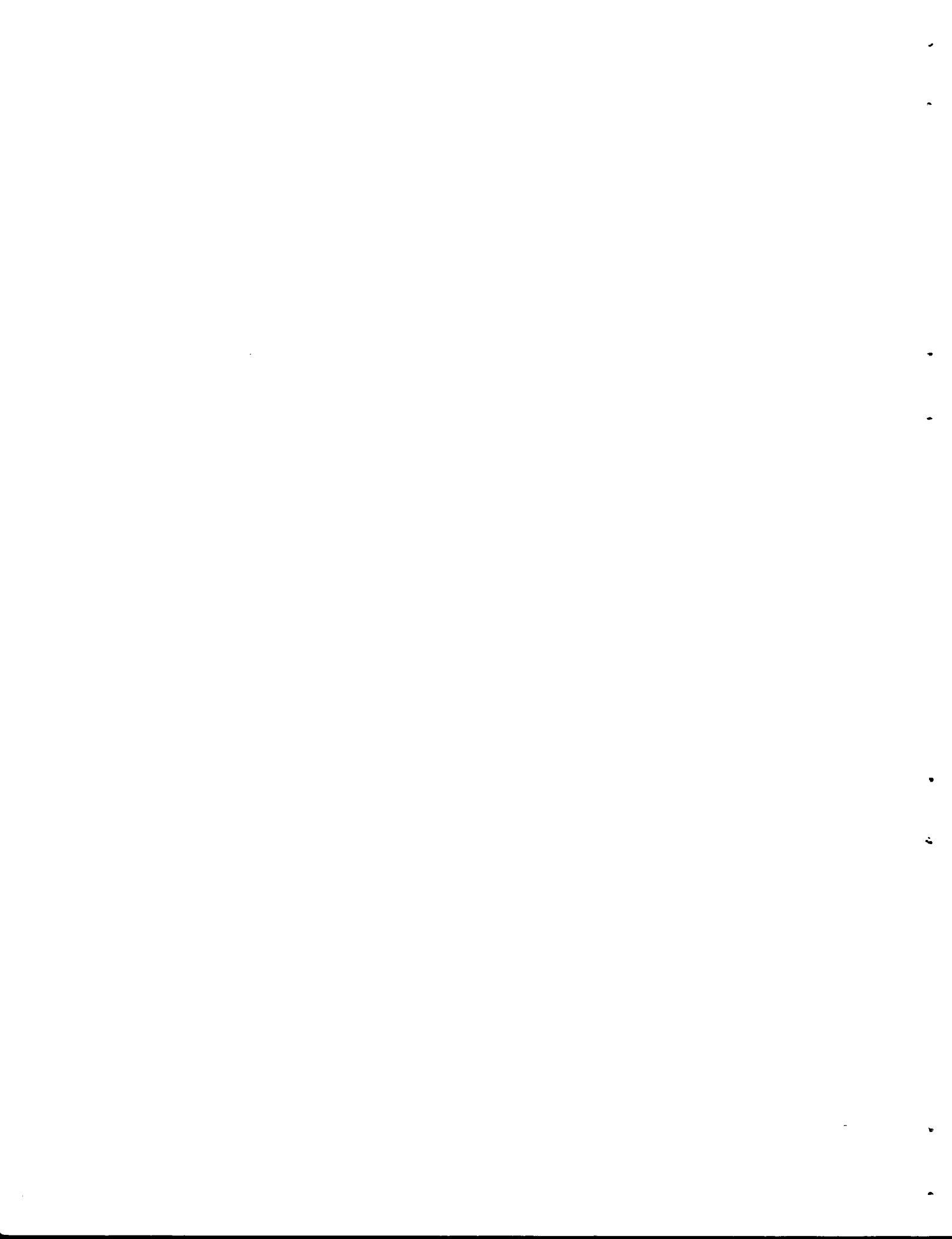
E	Efficiency of ion exchange expressed as a decimal fraction for a particular radioactive isotope
$E_e$	Effective threshold energy in Mev
$E_G$	Efficiency of vacuum degasification expressed as a decimal fraction for a particular radioactive isotope
$E_H$	Kinetic energy of a heavy fission fragment in Mev
$E_L$	Kinetic energy of a light fission fragment in Mev
$E_n$	Neutron energy in Mev
$E_R$	Energy of a recoiling atom in Mev
erf(x)	Error function of x
$E_T$	Threshold energy in Mev
$E_\beta$	Energy of a beta particle in Mev
$E_\gamma$	Gamma-ray energy in Mev
F	Number of gamma-rays of this energy emitted per disintegration expressed as a decimal fraction
f	Equal by definition to ct
G	Flow rate through a vacuum degasifier in milliliters per second divided by v
g	Equal by definition to bt
H	Equal by definition to Gt
h	Equal by definition to $(1 - E_g)(1 - f)(1 - E_{GH})e^{-\lambda t}$
I	Correction factor for absorption of gamma radiations in a source and/or any beta absorber used in a measurement
i	Empirical coefficient
J	Percent abundance of an isotope in an element divided by 100
j	Empirical coefficient
K	Henry's Law Constant in millimeters of mercury per mole fraction
L	Fraction of the total area under a low energy peak due to the spectrum of the low energy peak

M	Mass of a bombarded element in grams
$M_A$	Molecular weight of a solute A in grams per mole
$M_B$	Molecular weight of a solvent B in grams per mole
N	Number of active nuclei present per milliliter
$N_O$	Avogadro's number in reciprocal moles
$N_A$	Mole fraction of a solute in a solution
$N_T$	Number of target atoms
$N_{T0}$	Original number of target atoms at $T = 0$
n	Number of cycles
$n_A$	Number of moles of a solute
$n_B$	Number of moles of a solvent
$N_\gamma$	Number of disintegrations per second
P	Appropriate value for a peak-to-total ratio
$P_A$	Partial pressure of a solute in millimeters of mercury
p	Concentration of a solute in a solvent in parts per million
q	Constant
R	Recoil range in centimeters
$R_\beta$	Range of a beta particle in grams per square centimeter
r	Rate of production of a radioactive isotope in a coolant in atoms per second
$s(E_n)$	Number of fission neutrons per unit energy normalized to one fission neutron
$s_C(E_n)$	Represents the University of California Spectrum
$s_W(E_n)$	Represents the Watt Spectrum
T	Time in seconds for exposure to neutron flux
$T_1$	Decay time in seconds before entering a counting volume

$T_2$	Decay time in seconds after leaving a counting volume
$T_a$	Absolute temperature in degrees Kelvin
$T^*$	Decay time in seconds of a measured activity
$t$	Time required to complete one cycle in seconds
$t_R$	Average retention time of a coolant in a reactor core in seconds
$u$	Lower limit of integration in Mev
$V$	Volume within which the neutron flux is $\phi$ in cubic centimeters
$v$	Volume of a cooling system in milliliters
$w$	Upper limit of integration in Mev
$w_A$	Weight of a solute A in grams
$w_B$	Weight of a solute B in grams
$x$	Thickness of an absorber in centimeters
$Z$	Atomic number of a bombarded atom

#### Greek Letters

$\epsilon$	Total absolute detection efficiency for the source-detector geometry used
$\theta$	Angle between the direction an incoming neutron was moving in and the direction a recoiling atom, $A_1$ , is moving in
$\lambda$	Radioactive decay constant in reciprocal seconds
$\mu$	Coefficient of absorption in square centimeters per gram
$\rho$	Density of a bombarded material in grams per cubic centimeter
$\Sigma$	Macroscopic cross section for a process in units of reciprocal centimeters
$\sigma$	Microscopic cross section for a specific reaction in square centimeters
$\phi$	Neutron flux in neutrons per square centimeter per second



ORNL-3152  
 UC-4 - Chemistry  
 TID-4500 (16th ed.)

## INTERNAL DISTRIBUTION

- |  |                                 |
|--|---------------------------------|
| 1. Biology Library   | 48. G. W. Leddicotte            |
| 2-3. Central Research Library                                  | 49. T. A. Lincoln               |
| 4. Reactor Division Library                                    | 50. S. C. Lind                  |
| 5. ORNL - Y-12 Technical Library<br>Document Reference Section | 51. H. A. McClain (Y-12)        |
| 6-25. Laboratory Records Department                            | 52. K. Z. Morgan                |
| 26. Laboratory Records, ORNL R.C.                              | 53. J. P. Murray (K-25)         |
| 27. L. C. Bate   | 54. M. L. Nelson                |
| 28. D. S. Billington   | 55. D. Phillips                 |
| 29. G. E. Boyd   | 56. S. A. Reynolds              |
| 30. C. D. Cagle  | 57. J. M. Schreyer              |
| 31. A. E. Cameron  | 58. H. Schweinler               |
| 32. W. R. Casto  | 59. H. E. Seagren               |
| 33. C. E. Center   | 60. M. J. Skinner               |
| 34. L. T. Corbin   | 61. J. E. Strain                |
| 35. J. A. Cox  | 62. C. D. Susano                |
| 36. F. L. Culler   | 63. J. A. Swartout              |
| 37. F. F. Dyer   | 64. W. H. Tabor                 |
| 38. J. F. Emery  | 65. E. H. Taylor                |
| 39. L. G. Farrar   | 66-85. J. C. Ward               |
| 40. J. H. Frye, Jr.  | 86. A. M. Weinberg              |
| 41. J. H. Gillette   | 87. J. C. White                 |
| 42. J. Halperin  | 88. H. E. Zittel                |
| 43. A. Hollaender  | 89. N. H. Furman (consultant)   |
| 44. A. S. Householder  | 90. D. N. Hume (consultant)     |
| 45. R. G. Jordan (Y-12)  | 91. H. A. Laitinen (consultant) |
| 46. M. T. Kelley   | 92. C. E. Larson (consultant)   |
| 47. J. A. Lane   | 93. W. W. Meinke (consultant)   |
|  | 94. L. L. Merritt (consultant)  |

## EXTERNAL DISTRIBUTION

- 95-96. D. S. Anthony, ORINS
97. G. W. Reid, University of Oklahoma, Norman, Oklahoma
98. R. A. Howard, University of Oklahoma, Norman, Oklahoma
99. N. Fogel, University of Oklahoma, Norman, Oklahoma
100. J. R. Assenzo, University of Oklahoma, Norman, Oklahoma
101. R. Thompson, University of Oklahoma, Norman, Oklahoma
102. Division of Research and Development, AEC, ORO
103. Engineering Library, University of Oklahoma, Norman, Oklahoma
104. Physics Library, University of Oklahoma, Norman, Oklahoma
- 105-696. Given distribution as shown in TID-4500 (16th ed.) under Chemistry category (75 copies - OTS)